SIAM J. Applied Dynamical Systems
Vol. 18, No. 4, pp. 1798–1845

Stability Analysis of Line Patterns of an Anisotropic Interaction Model*

José A. Carrillo†, Bertram Düring‡, Lisa Maria Kreusser§, and Carola-Bibiane Schönlieb§

Abstract. Motivated by the formation of fingerprint patterns, we consider a class of interacting particle models with anisotropic, repulsive-attractive interaction forces whose orientations depend on an underlying tensor field. This class of models can be regarded as a generalization of a gradient flow of a nonlocal interaction potential which has a local repulsion and a long-range attraction structure. In addition, the underlying tensor field introduces an anisotropy leading to complex patterns which do not occur in isotropic models. Central to this pattern formation are straight line patterns. For a given spatially homogeneous tensor field, we show that there exists a preferred direction of straight lines, i.e., straight vertical lines can be stable for sufficiently many particles, while many other rotations of the straight lines are unstable steady states, both for a sufficiently large number of particles and in the continuum limit. For straight vertical lines we consider specific force coefficients for the stability analysis of steady states, show that stability can be achieved for exponentially decaying force coefficients for a sufficiently large number of particles, and relate these results to the Kücken–Champod model for simulating fingerprint patterns. The mathematical analysis of the steady states is completed with numerical results.

Key words. aggregation, swarming, pattern formation, dynamical systems

AMS subject classifications. 35B36, 35Q92, 70F10, 70F45, 82C22

DOI. 10.1137/18M1181638

1. Introduction.

Mathematical models for biological aggregation describing the collective behavior of large numbers of individuals have given us many tools to understand pattern formation in nature. Typical examples include models for explaining the complex phenomena observed in swarms of insects, flocks of birds, schools of fish, or colonies of bacteria; see, for instance, [7, 8, 12, 18, 24, 32, 33, 34, 35, 37, 45, 48, 49]. Some continuum models have

*Received by the editors June 18, 2018; accepted for publication (in revised form) by C. Topaz August 8, 2019; published electronically October 15, 2019.
https://doi.org/10.1137/18M1181638
Funding: The work of the first author was partially supported by the EPSRC through grant EP/P031587/1. The work of the second author was supported by the Leverhulme Trust research project grant "Novel discretizations for higher order nonlinear PDE" (RPG-2015-69). The work of the third author was supported by the UK Engineering and Physical Sciences Research Council (EPSRC) grant EP/L016516/1 and the German Academic Scholarship Foundation (Studienstiftung des Deutschen Volkes). The work of the fourth author was supported by the Leverhulme Trust project on breaking the non-convexity barrier, EPSRC grant EP/M00483X/1, the EPSRC Centre EP/N014588/1, the RISE projects CHiPS and NoMADS, the Cantab Capital Institute for the Mathematics of Information, and the Alan Turing Institute.
†Department of Mathematics, Imperial College London, London SW7 2AZ, UK (carrillo@imperial.ac.uk, http://wwwf.imperial.ac.uk/~jcarrill/).
‡Department of Mathematics, University of Sussex, Pevensey II, Brighton BN1 9QH, UK (b.during@sussex.ac.uk, http://users.sussex.ac.uk/~bd80/).
§Department of Applied Mathematics and Theoretical Physics (DAMTP), University of Cambridge, Cambridge, CB3 0WA, UK (L.M.Kreusser@damtp.cam.ac.uk, http://www.damtp.cam.ac.uk/user/lmk48/, C.B.Schoenlieb@damtp.cam.ac.uk, http://www.damtp.cam.ac.uk/user/cbs31/).

been derived from individual based descriptions [13, 14, 15, 16, 40, 52, 53, 56]; see also the reviews [25, 42], leading to an understanding of the stability of patterns at different levels [1, 11, 27, 28, 43].

A key feature of many of these models is that the communication between individuals takes place at different scales, i.e., each individual can interact not only with its neighbors but also with individuals further away. This can be described by short- and long-range interactions [8, 37, 45]. In most models the interactions are assumed to be *isotropic* for simplicity. However, pattern formation in nature is usually *anisotropic* [6]. Motivated by the simulation of fingerprint patterns we consider a class of interacting particle models with anisotropic interaction forces in this paper. In particular, these anisotropic interaction models capture important swarming behaviors, neglected in the simplified isotropic interaction model, such as anisotropic steady states.

The simplest form of isotropic interaction models is based on radial interaction potentials [4]. In this case one can consider the stationary points of the N-particle interaction energy

$$E(x_1, \dots, x_N) = \frac{1}{2N^2} \sum_{\substack{j,k=1 \\ k \neq j}}^{N} W(x_j - x_k).$$

Here, $W(d) = \overline{W}(|d|)$ denotes the radially symmetric interaction potential and $x_j = x_j(t) \in \mathbb{R}^n$ for $j = 1, \dots, N$ are the positions of the particles at time $t \geq 0$ [11, 43]. One can easily show that the associated gradient flow reads

$$\frac{\mathrm{d}x_j}{\mathrm{d}t} = \frac{1}{N} \sum_{\substack{k=1 \\ k \neq j}}^{N} F(x_j - x_k), \tag{1.1}$$

where $F(x_j - x_k)$ is a conservative force, aligned along the distance vector $x_j - x_k$ with $F(d) = -\nabla W(d)$. In many biological applications the number of interacting particles is large and one may consider the underlying continuum formulation of (1.1), which is known as the aggregation equation [9, 11, 43] and is of the form

$$\rho_t + \nabla \cdot (\rho u) = 0, \qquad u = -\nabla W * \rho, \tag{1.2}$$

where $u = u(t, x)$ is the macroscopic velocity field and $\rho = \rho(t, x)$ denotes the density of particles at location $x \in \mathbb{R}^n$ at time $t > 0$. The aggregation equation (1.2) has been studied extensively recently, mainly in terms of its gradient flow structure [2, 30, 31, 44, 54], the blow-up dynamics for fully attractive potentials [9, 10, 21, 29], and the rich variety of steady states for repulsive-attractive potentials [3, 4, 5, 8, 10, 19, 20, 22, 23, 26, 27, 28, 38, 39, 50, 55, 56].

In biological applications, the interactions determined by the force F or, equivalently, the interaction potential W, are usually described by short-range repulsion, preventing collisions between the individuals, as well as long-range attraction, keeping the swarm cohesive [46, 47]. In this case, the associated radially symmetric potentials $\overline{W}$ first decrease and then increase as a function of the radius. Due to the repulsive forces these potentials lead to possibly more steady states than the purely attractive potentials. In particular, these repulsive-attractive

potentials can be considered as a minimal model for pattern formation in large systems of individuals [4, 42] and the references therein.

Pattern formation in multiple dimensions is studied in [11, 43, 55, 56, 27] for repulsive-attractive potentials. The instabilities of the sphere and ring solutions are studied in [11, 55, 56]. The linear stability of ring equilibria is analyzed and conditions on the potential are derived to classify the different instabilities. A numerical study of the N-particle interaction model for specific repulsion-attraction potentials is also performed in [11, 43] leading to a wide range of radially symmetric patterns such as rings, annuli, and uniform circular patches, as well as more complex patterns. Based on this analysis the stability of flock solutions and mill rings in the associated second order model can be studied; see [1] and [28] for the linear and nonlinear stability of flocks, respectively.

In this work, we consider a generalization of the particle model (1.1) by introducing an anisotropy given by a tensor field T. This leads to an extended particle model of the form

$$\frac{\mathrm{d}x_j}{\mathrm{d}t} = \frac{1}{N}\sum_{\substack{k=1\\k\neq j}}^{N} F(x_j - x_k, T(x_j)), \tag{1.3}$$

where we prescribe initial data $x_j(0) = x_j^{in},\ j = 1,\dots,N$, for given scalars $x_j^{in},\ j = 1,\dots,N$. A special instance of this model has been introduced in [41] for simulating fingerprint patterns. The particle model in its general form (1.3) has been studied in [17, 36]. Here, the position of each of the N particles at time t is denoted by $x_j = x_j(t) \in \mathbb{R}^2,\ j = 1,\dots,N$, and $F(x_j - x_k, T(x_j))$ denotes the total force that particle k exerts on particle j subject to an underlying stress tensor field $T(x_j)$ at x_j, given by

$$T(x) := \chi s(x) \otimes s(x) + l(x) \otimes l(x) \in \mathbb{R}^{2,2} \tag{1.4}$$

for orthonormal vector fields $s = s(x)$ and $l = l(x) \in \mathbb{R}^2$ and $\chi \in [0,1]$. Here, the outer product $v \otimes w$ for two vectors $v, w \in \mathbb{R}^2$ equals the matrix multiplication vw^T and results in a matrix of size $\mathbb{R}^{2,2}$. The parameter χ introduces an anisotropy in the direction s in the definition of the tensor field.

For repulsive forces along s and short-range repulsive, long-range attractive forces along l the numerical simulations in [17] suggest that straight vertical line patterns formed by the interacting particles at positions x_j are stable for a certain spatially homogeneous tensor field, specified later. In this paper, we want to rigorously study this empirical observation by providing a linear stability analysis of such patterns where particles distribute equidistantly along straight lines.

The stability analysis of steady states of the particle model (1.3) is important for understanding the robustness of the patterns that arise from applying (1.3) for numerical simulation, for instance, as for its originally intended application to fingerprint simulation in [41]. Indeed, in what follows, we will show that for spatially homogeneous tensor fields T the solution formed by a number of vertical straight lines (referred to as ridges) is a stationary solution, whereas ridge bifurcations, i.e., a single ridge dividing into two ridges as typically appearing in fingerprint patterns, is not.

The aim of this paper is to prove that sufficiently large numbers of particles distributed equidistantly along straight vertical lines are stable steady states to the particle model (1.3) for short-range repulsive, long-range attractive forces along l and repulsive forces along s. All other rotations of straight lines are unstable steady states for this choice of force coefficients for a sufficiently large number of particles and for the continuum limit. We focus on this very simple class of steady states as a first step towards understanding stable formations that can be achieved by model (1.3). Note that the continuum straight line is a steady state of the associated continuum model

$$\partial_t \rho(t,x) + \nabla_x \cdot [\rho(t,x)\,(F(\cdot, T(x)) * \rho(t,\cdot))\,(x)] = 0 \qquad \text{in } \mathbb{R}_+ \times \mathbb{R}^2$$

(see [17]), but its asymptotic stability cannot be concluded from the linear stability analysis for finitely many particles.

The paper is organized as follows. In section 2 we describe a general formulation of an anisotropic interaction model, based on the model proposed by Kücken and Champod [41]. Section 3 is devoted to a high wave number stability analysis of line patterns for the continuum limit $N \to \infty$, including vertical, horizontal, and rotated straight lines for spatially homogeneous tensor fields. Due to the instability of arbitrary rotations except for vertical straight lines for the considered tensor field we focus on the stability analysis of straight vertical lines for particular forces for any $N \in \mathbb{N}$ in section 4. Section 5 illustrates the form of the steady states in the case the derived stability conditions are not satisfied.

2. Description of the model.

In this section, we describe a general formulation of the anisotropic microscopic model (1.3) and relate it to the Kücken–Champod particle model [41]. Kücken and Champod consider the particle model (1.3) where the total force F is given by

$$F(d(x_j,x_k), T(x_j)) = F_A(d(x_j,x_k), T(x_j)) + F_R(d(x_j,x_k)) \tag{2.1}$$

for the distance vector $d(x_j,x_k) = x_j - x_k \in \mathbb{R}^2$. Here, F_R denotes the repulsion force that particle k exerts on particle j and F_A is the attraction force particle k exerts on particle j. The repulsion and attraction forces are of the form

$$F_R(d = d(x_j,x_k)) = f_R(|d|)d \tag{2.2}$$

and

$$F_A(d = d(x_j,x_k), T(x_j)) = f_A(|d|)T(x_j)d, \tag{2.3}$$

respectively, with coefficient functions f_R and f_A, where, again, $d = d(x_j,x_k) = x_j - x_k \in \mathbb{R}^2$. Note that the repulsion and attraction force coefficients f_R, f_A are radially symmetric. The direction of the interaction forces is determined by the parameter $\chi \in [0,1]$ in the definition of T in (1.4). Motivated by plugging (1.4) into the definition of the total force (2.1), we consider a more general form of the total force, given by

$$F(d = d(x_j,x_k), T(x_j)) = f_s(|d|)(s(x_j)\cdot d)s(x_j) + f_l(|d|)(l(x_j)\cdot d)l(x_j), \tag{2.4}$$

where the total force is decomposed into forces along the direction s and along the direction l. In particular, the force coefficients in the Kücken–Champod model (1.3) with repulsive and attractive forces F_R and F_A in (2.2) and (2.3), respectively, can be recovered for

$$f_l(|d|) = f_A(|d|) + f_R(|d|) \quad \text{and} \quad f_s(|d|) = \chi f_A(|d|) + f_R(|d|).$$

Since a steady state of the particle model (1.3) for any spatially homogeneous tensor field $\tilde{T}$ can be regarded as a coordinate transform of the steady state of the particle model (1.3) for the tensor field T (see [17] for details), we restrict ourselves to the study of steady states for the spatially homogeneous tensor field T given by the orthonormal vectors $s = (0, 1)$ and $l = (1, 0)$, i.e.,

$$T = \begin{pmatrix} 1 & 0 \\ 0 & \chi \end{pmatrix}. \tag{2.5}$$

The total force in the Kücken–Champod model (2.1) and the generalized total force (2.4) reduce to

$$F(d) = \begin{pmatrix} (f_A(|d|) + f_R(|d|))\, d_1 \\ (\chi f_A(|d|) + f_R(|d|))\, d_2 \end{pmatrix} \tag{2.6}$$

and

$$F(d) = \begin{pmatrix} f_l(|d|) d_1 \\ f_s(|d|) d_2 \end{pmatrix} \quad \text{for } d = (d_1, d_2) \in \mathbb{R}^2, \tag{2.7}$$

respectively, for the spatially homogeneous tensor field T in (2.5).

In the following, we consider the particle model (1.3) on the torus $\mathbb{T}^2$ or, equivalently, on the unit square $[0, 1]^2$ with periodic boundary conditions. This can be achieved by considering the full force (2.7) on $[-0.5, 0.5]^2$, extending it periodically on $\mathbb{R}^2$, and requiring that the force coefficients are differentiable and vanish on $\partial[-0.5, 0.5]^2$ for physically realistic dynamics. That is, we use (2.7) to define its periodic extension $\bar{F}\colon \mathbb{R}^2 \to \mathbb{R}^2$ by

$$\begin{aligned} \bar{F}(d) &:= F(d) \quad \text{for } d \in [-0.5, 0.5]^2, \\ \bar{F}(d + k) &:= \bar{F}(d) \quad \text{for } d \in [-0.5, 0.5]^2, k \in \mathbb{Z}^2. \end{aligned} \tag{2.8}$$

Then, the particle model (1.3) can be rewritten as

$$\frac{\mathrm{d}x_j}{\mathrm{d}t} = \frac{1}{N} \sum_{\substack{k=1 \\ k \neq j}}^{N} \bar{F}(x_j - x_k) \tag{2.9}$$

for $x_j \in \mathbb{R}^2$, where the right-hand side can be regarded as the force acting on particle j. For physically realistic forces, the force $\bar{F}$ has to vanish for any $d \in \partial[-0.5, 0.5]^2$, implying that $f_l(0.5) = f_s(0.5) = 0$ for f_l, f_s in (2.7) and hence $f_l(|d|) = f_s(|d|) = 0$ for $d \in \mathbb{R}^2$ with $|d| = 0.5$. Thus, we require that $\bar{F}(d) = 0$ for all $d \in \partial[-0.5, 0.5]^2$ for physically relevant forces. To guarantee that the resulting force coefficient is differentiable which is required for the stability analysis we construct a differentiable approximation of the given force coefficient

f by considering $f(|d|)$ for $|d| \leq 0.5 - \epsilon$ for some $\epsilon > 0$, a cubic polynomial on $(0.5-\epsilon, 0.5)$, and the constant zero function for $|d| \geq 0.5$ such that the resulting function is continuously differentiable on $(0, \infty)$. Motivated by this, we also consider smaller values of the cutoff radius $R_c \in (0, 0.5]$ and adapt the force coefficients as

$$f^\epsilon(|d|) = \begin{cases} f(|d|), & |d| \in [0, R_c - \epsilon], \\ f'(R_c-\epsilon)\left(\frac{(|d|-R_c)^3}{\epsilon^2} + \frac{(|d|-R_c)^2}{\epsilon}\right) & \\ \quad + f(R_c-\epsilon)\left(2\frac{(|d|-R_c)^3}{\epsilon^3} + 3\frac{(|d|-R_c)^2}{\epsilon^2}\right), & |d| \in (R_c-\epsilon, R_c), \\ 0, & |d| \geq R_c. \end{cases} \tag{2.10}$$

Note that this definition results in a differentiable function whose absolute value and its derivative vanish for $|d| = R_c$. This is in analogy to the notion of cutoff and is only a small modification compared to the original definition provided $f(s)$ for $s \in (R_c - \epsilon, R_c)$ is of order $\mathcal{O}(\epsilon)$ and $f'(R_c - \epsilon)$ is of order $\mathcal{O}(1)$. In this case, both the original force coefficients and its adaptation f^ϵ are of order $\mathcal{O}(\epsilon)$ on $(R_c - \epsilon, R_c)$. Further note that the interaction forces on distances $|d| \ll R_c - \epsilon$ are significantly larger than on $(R_c - \epsilon, R_c)$ and, hence, the dynamics are mainly determined by interactions of range $|d| \ll R_c$. In particular, this allows us to replace f_l and f_s in (2.7) by differentiable approximations f_l^ϵ and f_s^ϵ, defined as in (2.10), if necessary.

Note that the assumption to consider the unit square $[0,1]^2$ with periodic boundary conditions is not restrictive and by rescaling in time our analysis extends to any domain $[0, \delta]^2$ with a cutoff radius $R_c \in (0, \frac{\delta}{2}]$ for $\delta \in \mathbb{R}_+$, where the cutoff of any force coefficient f is defined in (2.10).

The coefficient function f_R of the repulsion force F_R in (2.2) in the Kücken–Champod model is originally of the form

$$f_R(|d|) = (\alpha |d|^2 + \beta) \exp(-e_R |d|) \tag{2.11}$$

for $d \in \mathbb{R}^2$ and nonnegative parameters α, β, and e_R. The coefficient function f_A of the attraction force F_A in (2.3) is of the form

$$f_A(|d|) = -\gamma |d| \exp(-e_A |d|) \tag{2.12}$$

for $d \in \mathbb{R}^2$ and nonnegative constants γ and e_A. To be as close as possible to the work by Kücken and Champod [41] we assume that the total force (2.1) exhibits short-range repulsion and long-range attraction along l and one can choose the parameters as

$$\alpha = 270, \quad \beta = 0.1, \quad \gamma = 35, \quad e_A = 95, \quad e_R = 100, \quad \chi \in [0,1] \tag{2.13}$$

as proposed in [17]. Based on the adaptations of the force coefficients in (2.10), we consider the modified Kücken–Champod force coefficients in the following, given by

$$f_R^\epsilon(|d|) = \begin{cases} f_R(|d|), & |d| \in [0, R_c - \epsilon], \\ f_R'(R_c-\epsilon)\left(\frac{(|d|-R_c)^3}{\epsilon^2} + \frac{(|d|-R_c)^2}{\epsilon}\right) & \\ \quad + f_R(R_c-\epsilon)\left(2\frac{(|d|-R_c)^3}{\epsilon^3} + 3\frac{(|d|-R_c)^2}{\epsilon^2}\right), & |d| \in (R_c-\epsilon, R_c), \\ 0, & |d| \geq R_c \end{cases} \tag{2.14}$$

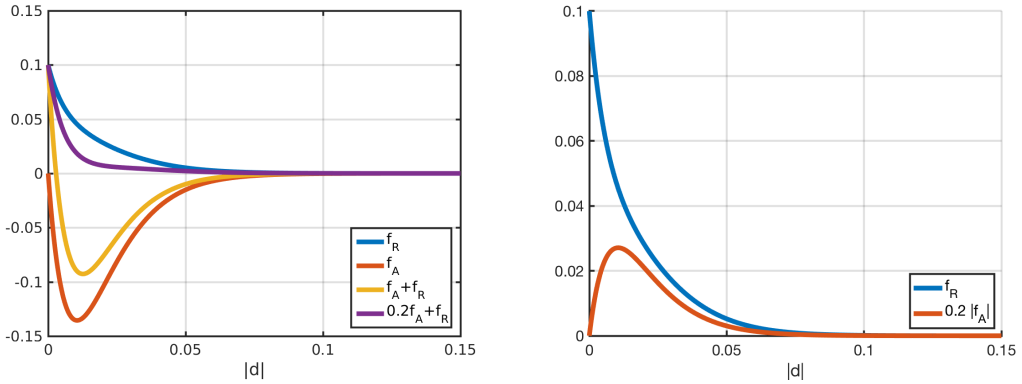

Figure 1. *Coefficients f_R in (2.11) and f_A in (2.12) of repulsion force (2.2) and attraction force (2.3), respectively, as well as the force coefficients along $s = (0,1)$ and $l = (1,0)$ (i.e., $f_A + f_R$ and $0.2f_A + f_R$) for parameter values in (2.13).*

and

$$f_A^\epsilon(|d|) = \begin{cases} f_A(|d|), & |d| \in [0, R_c - \epsilon], \\ f_A'(R_c-\epsilon)\left(\frac{(|d|-R_c)^3}{\epsilon^2} + \frac{(|d|-R_c)^2}{\epsilon}\right) & \\ \quad + f_A(R_c-\epsilon)\left(2\frac{(|d|-R_c)^3}{\epsilon^3} + 3\frac{(|d|-R_c)^2}{\epsilon^2}\right), & |d| \in (R_c-\epsilon, R_c), \\ 0, & |d| \geq R_c. \end{cases} \tag{2.15}$$

Here, f_R, f_A are very small in a neighborhood of the cutoff $R_c = 0.5$ for the parameters in (2.13) or, more generally, for e_R and e_A sufficiently large. Since the derivatives f_R' and f_A' also contain the exponential decaying terms $\exp(-e_R|d|)$ and $\exp(-e_A|d|)$, respectively, and are scaled by a factor $\mathcal{O}(\epsilon)$ in (2.14) and (2.15), respectively, the differences between f_R^ϵ and f_R, and f_A^ϵ and f_A, respectively, are very small compared to the size of the interaction forces at distances $|d| \ll R_c - \epsilon$ and the total force exerted on particle x_j, given by the right-hand side of (2.9). In particular, $f_R^\epsilon, f_A^\epsilon$ can be regarded as differentiable approximations of f_R, f_A.

For the particle model (2.9) with differentiable coefficient functions $f_R^\epsilon, f_A^\epsilon$ and parameters (2.13), we plot the original coefficient functions f_R, f_A of the total force (2.6) for a spatially homogeneous underlying tensor field T with $s = (0,1)$ and $l = (1,0)$ in Figure 1. However, note that $f_R \approx \lim_{\epsilon\to 0} f_R^\epsilon$ and $f_A \approx \lim_{\epsilon\to 0} f_A^\epsilon$. Moreover, we show the resulting coefficient functions $\chi f_A + f_R$ with $\chi = 0.2$ and $f_A + f_R$ along $s = (0,1)$ and $l = (1,0)$, respectively, in Figure 1. Note that the repulsive force coefficient f_R is positive and the attractive force coefficient f_A is negative. Repulsion dominates for short distances along l to prevent collisions of the particles. Besides, the total force exhibits long-range attraction along l whose absolute value decreases with the distance between particles. Along s, the particles are purely repulsive for $\chi = 0.2$ and the repulsion force gets weaker for longer distances.

3. Stability/Instability of straight lines.

In this section, we consider the total force $\bar{F}$ in (2.8), defined on $\mathbb{R}^2$ by periodic extension of F on $[-0.5, 0.5]^2$ in (2.7). This total force $\bar{F}$ can be described by (periodically extending) a short-range repulsive, long-range attractive force coefficient f_l along l and a purely repulsive force coefficient f_s along s. Without loss of

generality we may assume that the force coefficients f_l, f_s are differentiable since otherwise they may be replaced by $f_l^\epsilon, f_s^\epsilon$, defined as in (2.10) for given functions f_l, f_s. Motivated by this we require the following.

Assumption 3.1. Let f_l, f_s be continuously differentiable functions on $[0, \infty)$. Let f_s be purely repulsive, i.e., $f_s \geq 0$ with $f_s(0) > 0$ for $s \in [0, R_c)$ and $f_s(s) = 0$ for $s \geq R_c$, implying $\int_0^{R_c} f_s \, \mathrm{d}s > 0$. Further let f_l be short-range repulsive, long-range attractive with $f_l(R_c) = 0$.

As shown in [17] for the analysis of steady states with general spatially homogeneous tensor fields, it is sufficient to restrict ourselves to the spatially homogeneous tensor field T with $s = (0, 1)$ and $l = (1, 0)$ in the following.

3.1. Straight line. In this section, we consider line patterns as steady states which were observed in the numerical simulations in [17]. For $x_j \in \mathbb{R}^2, j = 1, \ldots, N$, evolving according to the particle model (2.9), we have

$$\frac{\mathrm{d}}{\mathrm{d}t} \sum_{j=1}^{N} x_j = 0,$$

implying that the center of mass is conserved. Hence, we can assume without loss of generality that the center of mass is in $\mathbb{Z}^2$. By identifying $\mathbb{R}^2$ with $\mathbb{C}$, we make the ansatz

$$\bar{x}_k = \frac{k}{N} \exp(i\theta)\ell(\theta), \quad k = 1, \ldots, N. \tag{3.1}$$

Here, θ denotes the angle of rotation. The length of the line pattern is denoted by $\ell = \ell(\theta) > 0$ and can be regarded as a multiplicative factor with $\ell(0) = \ell\left(\frac{\pi}{2}\right) = 1$ and $\ell\left(\frac{\pi}{4}\right) = \ell\left(\frac{3\pi}{4}\right) = \sqrt{2}$. Note that it is sufficient to restrict ourselves to $\theta \in [0, \pi)$ since ansatz (3.1) for θ and $\theta + k\pi$ with $k \in \mathbb{Z}$ leads to the same straight line after periodic extension on $\mathbb{R}^2$ and hence also on the torus $\mathbb{T}^2$. Depending on the choice of θ, ansatz (3.1) might lead to multiple windings on the torus $\mathbb{T}^2$. To guarantee that ansatz (3.1) satisfies the periodic boundary conditions, we require that the winding number of the straight lines in (3.1) is a natural number and hence we can restrict ourselves to ansatz (3.1) on the torus $\mathbb{T}^2$ for $\theta \in \mathcal{A}$, where

$$\begin{aligned} \mathcal{A} := &\left\{0, \frac{\pi}{4}, \frac{\pi}{2}, \frac{3\pi}{4}\right\} \cup \left\{\psi \in \left(0, \frac{\pi}{4}\right) \cup \left(\frac{3\pi}{4}, \pi\right) : \cot(\psi) \in \mathbb{Z}\right\} \\ &\cup \left\{\psi \in \left(\frac{\pi}{4}, \frac{3\pi}{4}\right) : \tan(\psi) \in \mathbb{Z}\right\}. \end{aligned} \tag{3.2}$$

Note that considering the torus $\mathbb{T}^2$ as the domain, i.e., the unit square with periodic boundary conditions or, equivalently, $\mathbb{R}^2$ by periodic extension, is not restrictive due to the discussion in section 2.

For a single vertical straight line we have $\theta = \frac{\pi}{2}$ and ansatz (3.1) reduces to

$$\bar{x}_k = \frac{k}{N} i, \quad k = 1, \ldots, N, \tag{3.3}$$

and for a horizontal line with $\theta = 0$ we have

$$\bar{x}_k = \frac{k}{N}, \quad k = 1, \ldots, N. \tag{3.4}$$

Note that the winding number is one for (3.1) with $\theta \in \{0, \frac{\pi}{4}, \frac{\pi}{2}, \frac{3\pi}{4}\}$, while the winding number is larger than one for $\theta \in \mathcal{A} \setminus \{0, \frac{\pi}{4}, \frac{\pi}{2}, \frac{3\pi}{4}\}$. Translations of the ansatz (3.1) result in steady states with a shifted center of mass. Besides, parallel equidistant straight line patterns, obtained from considering (3.1) for a fixed rotation angle (3.2) and certain translations, may also lead to steady states.

For equilibria $\bar{x}_j \in \mathbb{R}^2, j = 1, \dots, N$, to the particle model (2.9) we require that

$$\frac{1}{N} \sum_{\substack{k=1 \\ k \neq j}}^{N} \bar{F}(\bar{x}_j - \bar{x}_k, T) = 0 \quad \text{for all } j = 1, \dots, N.$$

Setting $\bar{x}_k$ for $k \in \mathbb{Z}$ as in (3.1), we have $\bar{F}(\bar{x}_j - \bar{x}_k) = \bar{F}(\bar{x}_j - \bar{x}_{k+nN})$ for $j, k = 1, \dots, N$ and any $n \in \mathbb{Z}$ by the periodicity of $\bar{F}$. Since the particles are uniformly distributed along straight lines by ansatz (3.1), it is sufficient to require

$$\sum_{k=1}^{N-1} \bar{F}(\bar{x}_N - \bar{x}_k, T) = 0 \tag{3.5}$$

for steady states. Note that $\bar{F}(\bar{x}_N - \bar{x}_k, T) = -\bar{F}(\bar{x}_N - \bar{x}_{N-k}, T)$ for $k = 1, \dots, \lceil N/2 \rceil - 1$ and for N even we have $\bar{F}(\bar{x}_N - \bar{x}_{N/2}, T) = 0$ by the definition of the cutoff R_c. Hence, (3.5) is satisfied for the ansatz (3.1) for $\theta \in \mathcal{A}$, provided the length $\ell(\theta)$ of the lines is set such that the particles are distributed uniformly along the entire axis of angle θ.

3.2. Stability conditions. In this section we derive stability conditions for equilibria of the particle model (2.9), based on a linearized stability analysis. The real parts of the eigenvalues of a stability matrix play a crucial role and we denote the real part of eigenvalue $\lambda \in \mathbb{C}$ by $\Re(\lambda)$ in the following.

Proposition 3.2. *For finite $N \in \mathbb{N}$, the steady state $\bar{x}_j$, $j = 1, \dots, N$, of the particle model (2.9) is asymptotically stable if the eigenvalues λ of the stability matrix*

$$M = M(j,m) = \big(I_1(j,m), \quad I_2(j,m)\big) \in \mathbb{C}^{2,2}, \tag{3.6}$$

satisfy $\Re(\lambda) < 0$ for all $j = 1, \dots, N$ and $m = 1, \dots, N-1$, where

$$\begin{aligned} I_1(j,m) &= \frac{1}{N} \sum_{k \neq j} \left(1 - \exp(im(\phi_k - \phi_j))\right) \frac{\partial \bar{F}}{\partial d_1}(\bar{x}_j - \bar{x}_k) \\ &= \frac{1}{N} \sum_{k \neq j} \left(1 - \exp\left(\frac{2\pi i m(k-j)}{N}\right)\right) \frac{\partial \bar{F}}{\partial d_1}(\bar{x}_j - \bar{x}_k), \\ I_2(j,m) &= \frac{1}{N} \sum_{k \neq j} \left(1 - \exp(im(\phi_k - \phi_j))\right) \frac{\partial \bar{F}}{\partial d_2}(\bar{x}_j - \bar{x}_k) \\ &= \frac{1}{N} \sum_{k \neq j} \left(1 - \exp\left(\frac{2\pi i m(k-j)}{N}\right)\right) \frac{\partial \bar{F}}{\partial d_2}(\bar{x}_j - \bar{x}_k) \end{aligned} \tag{3.7}$$

for $j = 1, \dots, N$ and $m = 1, \dots, N$.

Proof. Let $\bar{x}_j$, $j = 1, \dots, N$, denote a steady state of (2.9). We define the perturbation $g_j = g_j(t)$, $h_j = h_j(t) \in \mathbb{R}$ of $\bar{x}_j$ by

$$x_j = \bar{x}_j + \begin{pmatrix} g_j \\ h_j \end{pmatrix}, \quad j = 1, \dots, N.$$

Linearizing (2.9) around the steady state $\bar{x}_j$ gives

$$\frac{\mathrm{d}}{\mathrm{d}t}\begin{pmatrix} g_j \\ h_j \end{pmatrix} = \frac{1}{N}\sum_{k\neq j}(g_j - g_k)\frac{\partial \bar{F}}{\partial d_1}(\bar{x}_j - \bar{x}_k) + \frac{1}{N}\sum_{k\neq j}(h_j - h_k)\frac{\partial \bar{F}}{\partial d_2}(\bar{x}_j - \bar{x}_k). \tag{3.8}$$

We choose the ansatz functions

$$g_j = \zeta_g \left(\exp(im\phi_j) + \exp(-im\phi_j)\right), \quad h_j = \zeta_h \left(\exp(im\phi_j) + \exp(-im\phi_j)\right), \\ j = 1, \dots, N, \quad m = 1, \dots, N,$$

where $\zeta_g = \zeta_g(t), \zeta_h = \zeta_h(t)$, and $\phi_j = \frac{2\pi j}{N}$. Note that $g_j, h_j \in \mathbb{R}$ for all $j = 1, \dots, N$ and

$$\sum_{j=1}^{N} \exp(im\phi_j) = \sum_{j=1}^{N} \left(\exp\left(\frac{2\pi i m}{N}\right)\right)^j = \begin{cases} 0, & m = 1, \dots, N-1, \\ N, & m = N, \end{cases}$$

since ϕ_j are the roots of $r^N = 1$ and

$$\sum_{j=0}^{N-1} r^j = \frac{1 - r^N}{1 - r}.$$

This implies

$$\sum_{j=1}^{N} g_j(t) = \sum_{j=1}^{N} h_j(t) = \begin{cases} 0, & m = 1, \dots, N-1, \\ N, & m = N, \end{cases}$$

for all times $t \geq 0$, i.e., the center of mass of the perturbations g_j, h_j is preserved. We have

$$g_j - g_k = \zeta_g \left(\exp(im\phi_j) + \exp(-im\phi_j)\right)\left(1 - \exp(im(\phi_k - \phi_j))\right), \\ h_j - h_k = \zeta_h \left(\exp(im\phi_j) + \exp(-im\phi_j)\right)\left(1 - \exp(im(\phi_k - \phi_j))\right).$$

Plugging this into (3.8) and collecting like terms in $\exp(im\phi_j), \exp(-im\phi_j)$ results in

$$\frac{\mathrm{d}}{\mathrm{d}t}\begin{pmatrix} \zeta_g \\ \zeta_h \end{pmatrix} = \frac{\zeta_g}{N}\sum_{k\neq j}\left(1 - \exp(im(\phi_k - \phi_j))\right)\frac{\partial \bar{F}}{\partial d_1}(\bar{x}_j - \bar{x}_k) \\ + \frac{\zeta_h}{N}\sum_{k\neq j}\left(1 - \exp(im(\phi_k - \phi_j))\right)\frac{\partial \bar{F}}{\partial d_2}(\bar{x}_j - \bar{x}_k),$$

i.e.,

$$\frac{\mathrm{d}}{\mathrm{d}t}\begin{pmatrix}\zeta_g\\ \zeta_h\end{pmatrix} = M\begin{pmatrix}\zeta_g\\ \zeta_h\end{pmatrix}, \tag{3.9}$$

where the stability matrix $M \in \mathbb{C}^{2,2}$ is defined in (3.6). The ansatz $\zeta_g = \xi_g \exp(\lambda t)$, $\zeta_h = \xi_h \exp(\lambda t)$ solves the system (3.9) for any eigenvalue $\lambda \in \mathbb{C}$ of the stability matrix $M = M(j,m)$. Note that the stability matrix M is the zero matrix for $m = N$ and any $j = 1,\dots,N$. Hence, we have $\lambda = 0$ for $m = N$ and all $j = 1,\dots,N$, corresponding to translations along the vertical and horizontal axes. Thus, the straight line $\bar{x}_j, j = 1,\dots,N$, is stable if $\Re(\lambda) < 0$ for any $j = 1,\dots,N$ and $m = 1,\dots,N-1$. ∎

3.3. Stability of a single vertical straight line. To study the stability of a single vertical straight line of the form (3.3) we determine the eigenvalues of the stability matrix (3.6) and derive stability conditions for steady states $\bar{x}_j, j = 1,\dots,N$, satisfying (3.5). In the continuum limit $N \to \infty$ the steady state condition (3.5) becomes

$$\int_{-0.5}^{0.5} F((0,s),T)\,\mathrm{d}s = \int_{-0.5}^{0.5} \bar{F}((0,s),T)\,\mathrm{d}s = 0.$$

Due to the cutoff radius $R_c \in (0, 0.5]$ it is sufficient to require

$$\int_{-R_c}^{R_c} F((0,s),T)\,\mathrm{d}s = 0 \tag{3.10}$$

for equilibria. This condition is clearly satisfied for forces of the form (2.7) and in particular for forces of the form (2.6).

Theorem 3.3. *For finite $N \in \mathbb{N}$, the single vertical straight line (3.3) is an asymptotically stable steady state of the particle model (2.9) with total force (2.7) if $\Re(\lambda_{i,N}(m)) < 0$ for $i = 1,2$ and all $m = 1,\dots,N-1$, where the eigenvalues $\lambda_{i,N} = \lambda_{i,N}(m)$ of the stability matrix (3.6) are given by*

$$\begin{aligned}
\lambda_{1,N}(m) &= \frac{1}{N}\sum_{k=\lceil \frac{N}{2}\rceil}^{N-1+\lceil \frac{N}{2}\rceil} f_l(|d_{Nk}|)\left(1-\exp\left(\frac{2\pi i m k}{N}\right)\right),\\
\lambda_{2,N}(m) &= \frac{1}{N}\sum_{k=\lceil \frac{N}{2}\rceil}^{N-1+\lceil \frac{N}{2}\rceil} \left(f_s(|d_{Nk}|) + f_s'(|d_{Nk}|)|d_{Nk}|\right)\left(1-\exp\left(\frac{2\pi i m k}{N}\right)\right)
\end{aligned} \tag{3.11}$$

with

$$d_{Nk} = \begin{pmatrix}0\\ \frac{N-k}{N}\end{pmatrix}$$

for $k \in \mathbb{N}$. Denoting the cutoff radius by $R_c \in (0, 0.5]$, steady states satisfying the steady state condition (3.10) in the continuum limit $N \to \infty$ are unstable if $\Re(\lambda_i(m)) > 0$ for some $m \in \mathbb{N}$

and some $i \in \{1,2\}$*, where the eigenvalues* $\lambda_i = \lambda_i(m), i = 1,2$*, of the stability matrix* (3.6) *are given by*

$$\begin{aligned}\lambda_1(m) &= \int_{-R_c}^{R_c} f_l(|s|)\,(1-\exp(-2\pi i m s))\,\mathrm{d}s,\\ \lambda_2(m) &= \int_{-R_c}^{R_c} \left(f_s(|s|)+f_s'(|s|)|s|\right)(1-\exp(-2\pi i m s))\,\mathrm{d}s.\end{aligned} \tag{3.12}$$

In particular,

$$\begin{aligned}\Re(\lambda_1)(m) &= 2\int_0^{R_c} f_l(s)\,(1-\cos(-2\pi m s))\,\mathrm{d}s,\\ \Re(\lambda_2)(m) &= 2\int_0^{R_c} \left(f_s(s)+f_s'(s)s\right)(1-\cos(-2\pi m s))\,\mathrm{d}s.\end{aligned} \tag{3.13}$$

Proof. For the spatially homogeneous tensor field T, defined by $s=(0,1)$ and $l=(1,0)$, the derivatives of the total force (2.7) are given by

$$\frac{\partial \bar F}{\partial d_1}(d) = \begin{pmatrix} f_l(|d|)+f_l'(|d|)\frac{d_1^2}{|d|} \\ f_s'(|d|)\frac{d_1 d_2}{|d|}\end{pmatrix}, \qquad \frac{\partial \bar F}{\partial d_2}(d) = \begin{pmatrix} f_l'(|d|)\frac{d_1 d_2}{|d|} \\ f_s(|d|)+f_s'(|d|)\frac{d_2^2}{|d|}\end{pmatrix} \tag{3.14}$$

for $d=(d_1,d_2)\in[-0.5,0.5]^2$ and its periodic extension $\frac{\partial \bar F}{\partial d_i}(d+k) = \frac{\partial \bar F}{\partial d_i}(d)$ for $i=1,2$, $d\in[-0.5,0.5]^2$, and $k\in\mathbb{Z}^2$. Note that f_l, f_s are differentiable due to the smoothing assumptions at the cutoff R_c in (2.10) and their derivatives vanish for $d\in[-0.5,0.5]^2$ with $|d|\geq R_c$. Using ansatz (3.3) for a single vertical straight line, we obtain

$$\begin{aligned}\frac{\partial \bar F}{\partial d_1}(d_{jk}) &= \begin{pmatrix} f_l(|d_{jk}|) \\ 0\end{pmatrix},\\ \frac{\partial \bar F}{\partial d_2}(d_{jk}) &= \begin{pmatrix} 0 \\ f_s(|d_{jk}|)+f_s'(|d_{jk}|)|d_{jk}|\end{pmatrix}\end{aligned} \tag{3.15}$$

for $d_{jk}\in[-0.5,0.5]^2$ and note that $\frac{\partial \bar F}{\partial d_i}(d_{jk}) = \frac{\partial \bar F}{\partial d_i}(d_{j,k+nN})$ for $i=1,2$, $j,k=1,\dots,N$, and $n\in\mathbb{N}$. This implies that the particles along the straight vertical line are indistinguishable and it suffices to consider $j=N$. The entries (3.7) of the stability matrix (3.6) are given by

$$\begin{aligned}I_1(m) &= \frac{1}{N}\sum_{k=1}^{N}\left(1-\exp\left(\frac{2\pi i m k}{N}\right)\right)\frac{\partial \bar F}{\partial d_1}(d_{Nk}),\\ I_2(m) &= \frac{1}{N}\sum_{k=1}^{N}\left(1-\exp\left(\frac{2\pi i m k}{N}\right)\right)\frac{\partial \bar F}{\partial d_2}(d_{Nk}).\end{aligned}$$

Note that for $k=\lceil\frac{N}{2}\rceil,\dots,N$, we have $d_{Nk}\in\{0\}\times[0,0.5]\subset[-0.5,0.5]^2$, implying that the derivatives of $\bar F$ are given by (3.15), where $\bar F(d_{N,\lceil\frac{N}{2}\rceil})=0$ by the definition of the cutoff R_c for N even. Since $\frac{\partial \bar F}{\partial d_i}(d_{Nk}) = \frac{\partial \bar F}{\partial d_i}(d_{N,N+k})$ for $i=1,2$, $k=1,\dots,\lceil N/2\rceil-1$, and

$d_{N,N+k} \in \{0\} \times (-0.5, 0) \subset [-0.5, 0.5]^2$, we can replace the sum over $k \in \{1, \dots, N\}$ by the sum over $k \in \{\lceil \frac{N}{2} \rceil, \dots, N - 1 + \lceil \frac{N}{2} \rceil\}$, resulting in

$$
\begin{aligned}
I_1(m) &= \frac{1}{N} \sum_{k=\lceil \frac{N}{2} \rceil}^{N-1+\lceil \frac{N}{2} \rceil} \left(1 - \exp\left(\frac{2\pi i m k}{N}\right)\right) \frac{\partial \bar{F}}{\partial d_1}\left(d_{Nk}\right), \\
I_2(m) &= \frac{1}{N} \sum_{k=\lceil \frac{N}{2} \rceil}^{N-1+\lceil \frac{N}{2} \rceil} \left(1 - \exp\left(\frac{2\pi i m k}{N}\right)\right) \frac{\partial \bar{F}}{\partial d_2}\left(d_{Nk}\right).
\end{aligned} \tag{3.16}
$$

Note that the stability matrix (3.6) is a diagonal matrix whose eigenvalues are the nontrivial entries in (3.16) and are given by (3.11). Since the sums in (3.16) are Riemannian sums, we can pass to the continuum limit $N \to \infty$. Note that $\frac{k}{n} \in [0.5, 1.5]$ for $k \in \{\lceil \frac{N}{2} \rceil, \dots, N - 1 + \lceil \frac{N}{2} \rceil\}$ appears in the entries of the stability matrix (3.16). For passing to the limit $N \to \infty$ in (3.16), we consider the domain of integration $[0.5, 1.5]$ and do a change of variables resulting in

$$
\begin{aligned}
I_i(m) &= \int_{0.5}^{1.5} \frac{\partial \bar{F}}{\partial d_i}\left((0, 1-s)\right)\left(1 - \exp\left(2\pi i m s\right)\right) \mathrm{d}s = \int_{-0.5}^{0.5} \frac{\partial \bar{F}}{\partial d_i}\left((0, s)\right)\left(1 - \exp\left(-2\pi i m s\right)\right) \mathrm{d}s \\
&= \int_{-0.5}^{0.5} \frac{\partial F}{\partial d_i}\left((0, s)\right)\left(1 - \exp\left(-2\pi i m s\right)\right) \mathrm{d}s
\end{aligned}
$$

for $i = 1, 2$ and all $m \in \mathbb{N}$. Clearly the stability matrix (3.6) with entries $I_i, i = 1, 2$, is again a diagonal matrix and the eigenvalues $\lambda_i = \lambda_i(m), i = 1, 2$, in (3.12) are given by the diagonal entries of the stability matrix (3.6). ∎

Remark 3.4. In Theorem 3.3 we study the stability of the straight vertical line for the dynamical system (2.9) for a finite number of particles N, where the differentiability of $\bar{F}$ at the cutoff R_c is necessary for the definition of the eigenvalues in the discrete setting in (3.11). Note that we cannot conclude stability/instability if $\Re(\lambda_i(m)) \leq 0$ for $i = 1, 2$ and all $m = 1, \dots, N - 1$. By the assumptions on the force coefficients f_s, f_l in Assumption 3.1 we can pass to the continuum limit $N \to \infty$ in the definition of the eigenvalues of the stability matrix and study the stability of the steady states of the particle model (2.9) in the continuum limit $N \to \infty$. If there exists $m \in \mathbb{N}$ for some $i \in \{1, 2\}$ such that $\Re(\lambda_i(m)) > 0$, then the steady state is unstable in the continuum limit. However, if $\Re(\lambda_i(m)) \leq 0$ for $i \in \{1, 2\}$ and all $m \in \mathbb{N}$ stability/instability of the steady state cannot be concluded since it is difficult to give general conditions for $\Re(\lambda_i(m)) \to \sigma$ as $m \to \infty$ with $\sigma = 0$ or $\sigma \in \mathbb{R}_- \backslash \{0\}$. If $\sigma = 0$, we cannot say anything about the stability/instability of the steady state in the continuum setting; see also similar discussions for the stability/instability of delta-rings in the continuum setting in [51] and the discussion after Theorem 2.1 in [11]. In particular, linear stability for any $N \in \mathbb{N}$ is not sufficient to conclude stability in the continuum setting.

Note that the asymmetry in the definition of the eigenvalues (3.13) is due to the asymmetric steady states in (3.3). For $f = f_s = f_l$ the total force in (2.7) simplifies to $F(d) = f(|d|)d$ for $d = (d_1, d_2) \in [-0.5, 0.5]^2$. In this case, the gradient of $F = (F_1, F_2)$ is a symmetric matrix

(compare (3.14)) and, hence, the eigenvalues of the stability matrix are real. Since

$$\frac{\partial F_1}{\partial d_2} = \frac{\partial F_2}{\partial d_1}$$

there exists a radially symmetric potential $W(d) = w(|d|)$ such that $F = -\nabla W$ on $[-0.5, 0.5]^2$. Hence, the stability conditions can be derived in terms of the potential w and we have

$$\operatorname{trace}(\nabla F(d)) = f'(|d|)|d| + 2f(|d|) = -\Delta w(|d|) = \lambda_1 + \lambda_2$$

for $d \in [-0.5, 0.5]^2$ and the periodic extension $\bar{F}$ of F can be considered on $\mathbb{R}^2$. For $f_s = f_l$ and radially symmetric steady states, this leads to identical conditions for both eigenvalues λ_k, $k = 1, 2$. For the analysis of these symmetric steady states, however, it is helpful to consider an appropriate coordinate system such as polar coordinates for ring steady states as in [11].

Note that the stability conditions for steady states depend on the choice of the coordinate system. Considering derivatives with respect to the coordinate axes as in (3.14) seems to be the natural choice for straight line patterns, in contrast to polar coordinates as in [11].

In the following, we investigate the high wave number stability of straight line patterns for the particle model (2.9), i.e., the stability of straight vertical lines as $m \to \infty$. This can be studied by considering the limit $m \to \infty$ of the eigenvalues (3.12) of the stability matrix (3.6) associated with the dynamical system (3.9).

Proposition 3.5. *Suppose that the coefficient functions f_s and f_l are continuously differentiable on $[0, +\infty)$ with $f_s(|d|) = f_l(|d|) = 0$ for $|d| \geq R_c$ and $f_s \geq 0$. The condition*

$$\int_0^{R_c} f_l(s)\,\mathrm{d}s \leq 0 \quad \text{and} \quad f_s(R_c) = 0 \tag{3.17}$$

is necessary for the high wave number stability of the single straight vertical line (3.3), i.e., (3.17) is necessary for the stability of the straight vertical line for any $N \in \mathbb{N}$ and in the continuum limit $N \to \infty$.

Proof. The eigenvalues (3.12) of the stability matrix (3.6) associated with the equilibrium of a single vertical straight line are of the form

$$\begin{aligned}\lambda(m) &= \int_{-R_c}^{R_c} f(|s|)(1 - \exp(-2\pi i m s))\,\mathrm{d}s \\ &= 2\int_0^{R_c} f(s)\,\mathrm{d}s - \frac{1}{2\pi i m}\int_{-R_c}^{R_c} f'(|s|)\exp(-2\pi i m s)\,\mathrm{d}s \\ &\quad + \frac{1}{2\pi i m} f(R_c)\left(\exp(-2\pi i m R_c) - \exp(2\pi i m R_c)\right)\end{aligned}$$

for a function $f\colon \mathbb{R}_+ \to \mathbb{R}$ with $f(|d|) = 0$ for $|d| \geq R_c$. For high wave number stability we require

$$\int_0^{R_c} f(s)\,\mathrm{d}s \leq 0 \qquad \text{and} \qquad |f'| \text{ is integrable on } [0, R_c].$$

Then, using the definition of the eigenvalues (3.12) this leads to the conditions

$$\int_0^{R_c} f_l(s)\,\mathrm{d}s \le 0 \qquad \text{and} \qquad \int_0^{R_c} f_s(s) + f_s'(s)s\,\mathrm{d}s \le 0. \tag{3.18}$$

Integration by parts of the second condition in (3.18) leads to $f_s(R_c) \le 0$ and the conditions in (3.17) result from f_s being repulsive, i.e., $f_s \ge 0$. ∎

Remark 3.6. The necessary condition $f_s(R_c) = 0$ in (3.17) for a stable straight vertical line is equivalent to the eigenvalue associated with f_s to be equal to zero in the high wave number limit. Hence, stability/instability of straight vertical lines cannot be concluded in the continuum limit $N \to \infty$ from the linear stability analysis.

The first condition in (3.17) implies that the total attractive force over its entire range is larger than the total repulsive force along l. The second condition in (3.17) implies that for high wave stability we require the total force at the cutoff radius R_c should not be repulsive along s which is identical to the assumptions on the cutoff in (2.10).

In comparison with the high wave number conditions in (3.18) in the proof of Proposition 3.5 the integrands for the stability conditions are multiplied by a factor

$$\Re(1 - \exp(-2\pi i m s)) = 1 - \cos(2\pi m s) \in [0, 2].$$

Even if the necessary conditions for high wave number stability (3.17) are satisfied, this does not guarantee that $\Re(\lambda_1(m)), \Re(\lambda_2(m)) \le 0$ for all $m \in \mathbb{N}$ and hence necessary stability conditions for the single vertical straight line might not be satisfied for all $m \in \mathbb{N}$.

The general stability conditions for straight vertical lines can be obtained from the real parts of the eigenvalues (3.12) of the stability matrix (3.6). The conditions (3.17) suggest that stability of the straight line is possible for particular force coefficient choices. This will be investigated in section 4.

Remark 3.7. Note that differentiable approximations $f_R^\epsilon, f_A^\epsilon$ of the force coefficients f_R and f_A in the Kücken–Champod model are defined in (2.14) and (2.15), respectively. Setting $f_l^\epsilon := f_A^\epsilon + f_R^\epsilon$ and $f_s^\epsilon := \chi f_A^\epsilon + f_R^\epsilon$ for some $0 < \epsilon \ll R_c$ and a parameter $\chi \in [0, 1]$ such that $f_s \ge 0$ on $[0, R_c)$, we consider $f_l^\epsilon, f_s^\epsilon$ instead of f_l, f_s in the definition of the real parts of the eigenvalues (3.13). We obtain the following for the real parts of the eigenvalues of the stability matrix (3.6) in the Kücken–Champod model with total force (2.6) and the spatially homogeneous tensor field T in (2.5):

$$\Re(\lambda_1(m)) = 2\int_0^{R_c} (f_A^\epsilon(s) + f_R^\epsilon(s))\,(1 - \cos(-2\pi m s))\,\mathrm{d}s,$$
$$\Re(\lambda_2(m)) = 2\int_0^{R_c} \left(\chi f_A^\epsilon(s) + f_R^\epsilon(s) + \chi s (f_A^\epsilon)'(s) + s(f_R^\epsilon)'(s)\right)(1 - \cos(-2\pi m s))\,\mathrm{d}s.$$

The necessary stability condition (3.17) implies that $f_s^\epsilon(R_c) = \chi f_A^\epsilon(R_c) + f_R^\epsilon(R_c) = 0$, consistent with the definition of the force coefficients (2.14) and (2.15) in the Kücken–Champod model. Hence, the necessary condition (3.17) for high wave number stability of a straight vertical line is satisfied in this case.

3.4. Instability of a single horizontal straight line. In this section we investigate the stability of a single horizontal straight line given by the ansatz (3.4) which follows from (3.1) with $\theta = 0$.

Theorem 3.8. *For $N \in \mathbb{N}$ sufficiently large and in the continuum limit $N \to \infty$, the single horizontal straight line (3.4) is an unstable steady state to the particle model (2.9) for any choice of force coefficients f_s and f_l of the total force (2.7), provided the total force is purely repulsive along s on $[0, R_c)$.*

Proof. For a single horizontal straight line, we have

$$d_{jk} = \bar{x}_j - \bar{x}_k = \begin{pmatrix} \frac{j-k}{N} \\ 0 \end{pmatrix}$$

and the derivatives of the total force are given by

$$\frac{\partial}{\partial d_1}\bar{F}(d_{jk}) = \begin{pmatrix} f_l(|d_{jk}|) + f_l'(|d_{jk}|)|d_{jk}| \\ 0 \end{pmatrix},$$
$$\frac{\partial}{\partial d_2}\bar{F}(d_{jk}) = \begin{pmatrix} 0 \\ f_s(|d_{jk}|) \end{pmatrix}$$

for $d_{jk} \in [-0.5, 0.5]^2$. Similarly as in section 3.3 one can show that the eigenvalues $\lambda_1 = \lambda_1(m)$, $\lambda_2 = \lambda_2(m)$ of the stability matrix (3.6) are given by

$$\lambda_1(m) = 2\int_0^{R_c} \left(f_l(s) + f_l'(s)s\right)\left(1 - \exp\left(-2\pi i m s\right)\right) \mathrm{d}s,$$
$$\lambda_2(m) = 2\int_0^{R_c} f_s(s)\left(1 - \exp\left(-2\pi i m s\right)\right) \mathrm{d}s$$

for a cutoff radius $R_c \in (0, 0.5]$. For high wave number stability we require

$$f_l(R_c) = \frac{1}{R_c}\int_0^{R_c} f_l(s) + f_l'(s)s \,\mathrm{d}s \le 0 \qquad \text{and} \qquad \int_0^{R_c} f_s(s)\,\mathrm{d}s \le 0.$$

The forces are assumed to be purely repulsive along s up to the cutoff R_c, i.e., $f_s > 0$ on $[0, R_c)$, implying

$$\int_0^{R_c} f_s(s)\,\mathrm{d}s > 0.$$

Hence, the single horizontal straight line is high wave number unstable. ∎

3.5. Instability of rotated straight line patterns. In this section we consider the ansatz (3.1) where the angle of rotation θ satisfies (3.2), resulting in rotated straight line patterns. The entries of the stability matrix (3.6) are given by

$$I_1(m) = 2\int_0^{R_c} \frac{\partial \bar{F}}{\partial d_1}\left(\left(s\cos\left(\theta\right), s\sin\left(\theta\right)\right)\right)\left(1 - \exp\left(-2\pi i m s\right)\right) \mathrm{d}s,$$
$$I_2(m) = 2\int_0^{R_c} \frac{\partial \bar{F}}{\partial d_2}\left(\left(s\cos\left(\theta\right), s\sin\left(\theta\right)\right)\right)\left(1 - \exp\left(-2\pi i m s\right)\right) \mathrm{d}s,$$

where the derivatives of the total force can easily be determined by

$$\frac{\partial}{\partial d_1}\bar{F}(d) = \begin{pmatrix} f_l(|d|) + f_l'(|d|)\frac{d_1^2}{|d|} \\ f_s'(|d|)\frac{d_1 d_2}{|d|} \end{pmatrix}, \qquad \frac{\partial}{\partial d_2}\bar{F}(d) = \begin{pmatrix} f_l'(|d|)\frac{d_1 d_2}{|d|} \\ f_s(|d|) + f_s'(|d|)\frac{d_2^2}{|d|} \end{pmatrix},$$

$d \in [-0.5, 0.5]^2$ with the cutoff radius $R_c \in (0, 0.5]$. In particular, the stability matrix (3.6) is no longer a diagonal matrix in general. To show that the rotated straight line pattern is unstable for $\theta \in (0, \pi) \setminus [\phi, \pi - \phi]$ for some $\phi \in (0, \frac{\pi}{2})$ and $N \in \mathbb{N}$ sufficiently large and in the continuum limit $N \to \infty$, it is sufficient to consider the high frequency wave limit and show high wave number instability. Denoting the entries of I_k by I_{k1} and I_{k2} for $k = 1, 2$ with $M = (I_1, I_2)$ the high-frequency limit leads to

(3.19)
$$I_{11} = 2\int_0^{R_c} f_l(s)\,\mathrm{d}s + 2\int_0^{R_c} f_l'(s)s\cos^2(\theta)\,\mathrm{d}s, \qquad I_{12} = 2\int_0^{R_c} f_s'(s)s\sin(\theta)\cos(\theta)\,\mathrm{d}s,$$
$$I_{21} = 2\int_0^{R_c} f_l'(s)s\sin(\theta)\cos(\theta)\,\mathrm{d}s, \qquad I_{22} = 2\int_0^{R_c} f_s(s)\,\mathrm{d}s + 2\int_0^{R_c} f_s'(s)s\sin^2(\theta)\,\mathrm{d}s.$$

Here, $I_{12} = I_{21} = 0$ for $\theta = 0$ and $\theta = \frac{\pi}{2}$, i.e., for the straight horizontal and the straight vertical lines, respectively. Hence, the eigenvalues of the stability matrix are given by I_{11} and I_{22} in this case whose value are given by

$$I_{11} = 2R_c f_l(R_c), \quad I_{22} = 2\int_0^{R_c} f_s(s)\,\mathrm{d}s$$

for $\theta = 0$ and

$$I_{11} = 2\int_0^{R_c} f_l(s)\,\mathrm{d}s, \quad I_{22} = 2R_c f_s(R_c)$$

for $\theta = \frac{\pi}{2}$. This leads to the necessary conditions for high wave number stability for $\theta = \frac{\pi}{2}$ in (3.17), while due to Assumption 3.1 we obtain instability of the straight horizontal line.

Note that for any $\theta \in [0, \pi)$ the eigenvalues $\lambda_k, k = 1, 2$, are either real or complex conjugated and thus the sum and the product of λ_k are real. The condition $\Re(\lambda_k) \le 0, k = 1, 2$, is equivalent to $\mathrm{trace}(M) = \lambda_1 + \lambda_2 \le 0$ and $\det(M) = \lambda_1\lambda_2 \ge 0$. Hence, we require, for the stability of the rotated straight line,

$$I_{11} + I_{22} \le 0 \quad \text{and} \quad I_{11}I_{22} - I_{12}I_{21} \ge 0. \tag{3.20}$$

For showing the instability of the rotated straight line with angle of rotation $\theta \in (0, \pi) \setminus [\phi, \pi - \phi]$ for some $\phi \in (0, \frac{\pi}{2})$ we show that the two conditions in (3.20) cannot be satisfied simultaneously in this case.

Theorem 3.9. *For $N \in \mathbb{N}$ sufficiently large and in the continuum limit $N \to \infty$, the single straight line (3.1) where the angle of rotation $\theta \in (0, \pi) \setminus [\phi, \pi - \phi]$ for some $\phi \in (0, \frac{\pi}{2})$ satisfies (3.2) is an unstable steady state to the particle model (2.9) for any force coefficients f_s and f_l satisfying the general conditions for force coefficients in Assumption 3.1 and the conditions in (3.17).*

Proof. Note that we have

$$\int_0^{R_c} f_s'(s) s \sin^2(\theta)\,\mathrm{d}s = \sin^2(\theta)\left(f_s(R_c)R_c - \int_0^{R_c} f_s(s)\,\mathrm{d}s\right)$$

by integration by parts. For $\theta = 0$ and $f_l(R_c) = 0$ we have

$$I_{11} + I_{22} = 2R_c f_l(R_c) + 2\int_0^{R_c} f_s(s)\,\mathrm{d}s > 0,$$

while for $\theta = \frac{\pi}{2}$ we have

$$I_{11} + I_{22} = 2R_c f_s(R_c) + 2\int_0^{R_c} f_l(s)\,\mathrm{d}s \leq 0$$

by (3.17). Hence, there exists $\phi \in (0, \frac{\pi}{2})$ such that $I_{11} + I_{22} > 0$ on $(0, \phi)$. Since $\cos^2(\theta) = \cos^2(\pi - \theta)$ and $\sin^2(\theta) = \sin^2(\pi - \theta)$ we have $I_{11} + I_{22} > 0$ on $(\pi - \phi, \pi)$, implying that stability may only be possible on $[\phi, \pi - \phi]$. ∎

4. Stability of vertical lines for particular force coefficients. We have investigated the high wave number stability for $m \to \infty$ in section 3. Since only vertical straight lines for the considered spatially homogeneous tensor field T in (2.5) can lead to stable steady states for any $N \in \mathbb{N}$ we restrict ourselves to vertical straight lines in the following. As a next step towards proving stability we now consider the stability for fixed modes $m \in \mathbb{N}$.

Due to the form of the eigenvalues in (3.12) no general stability result for the single straight vertical line for the particle system (2.9) with arbitrary force coefficients f_s and f_l satisfying Assumption 3.1 can be derived. Thus, additional assumptions on the force coefficients are necessary.

4.1. Linear force coefficients. To study the stability of the single straight vertical line for any $N \in \mathbb{N}$, we consider linear force coefficients satisfying Assumption 3.1. To guarantee that the force coefficient is differentiable, required for using the results from section 3, we consider the differentiable adaptation (2.10) for a given linear force coefficient, leading to a linear force coefficient on $[0, R_c - \epsilon]$ for some $\epsilon > 0$, a cubic polynomial on $(R_c - \epsilon, R_c)$, and the constant zero function for $|d| \geq R_c$. This leads to the following conditions.

Assumption 4.1. For any $\epsilon > 0$ with $\epsilon \ll R_c$, we assume that the force coefficients are linear on $[0, R_c - \epsilon]$, i.e.,

(4.1)

$$f_l^\epsilon(|d|) := \begin{cases} a_l|d| + b_l, & |d| \in [0, R_c - \epsilon], \\ (2b_l + 2R_c a_l - a_l\epsilon)\frac{(|d|-R_c)^3}{\epsilon^3} + (3b_l + 3R_c a_l - 2a_l\epsilon)\frac{(|d|-R_c)^2}{\epsilon^2}, & |d| \in (R_c - \epsilon, R_c), \\ 0, & |d| \geq R_c, \end{cases}$$

$$f_s^\epsilon(|d|) := \begin{cases} a_s|d| + b_s, & |d| \in [0, R_c - \epsilon], \\ (2b_s + 2R_c a_s - a_s\epsilon)\frac{(|d|-R_c)^3}{\epsilon^3} + (3b_s + 3R_c a_s - 2a_s\epsilon)\frac{(|d|-R_c)^2}{\epsilon^2}, & |d| \in (R_c - \epsilon, R_c), \\ 0, & |d| \geq R_c, \end{cases}$$

for constants a_l, a_s, b_l, b_s. Since f_l^ϵ and f_s^ϵ are short-range repulsive, we require

$$b_l > 0, \quad b_s > 0.$$

Besides, for physically realistic force coefficients the absolute values of f_l^ϵ and f_s^ϵ are decaying, i.e.,

$$a_l < 0, \quad a_s < 0.$$

Note that for the short-range repulsive, long-range attractive force coefficient f_l, we have $a_l R_c + b_l < 0$ and in particular $a_l R_c + b_l$ is of order $\mathcal{O}(1)$. Hence, the adaptation f_l^ϵ of f_l for f_l linear is not negligible. However, due to the concentration of particles along a straight vertical line the adaptation f_l^ϵ acting along the vertical axis does not influence the overall dynamics provided $0 < \epsilon \ll R_c$. For the force coefficient f_s, the adaption f_s^ϵ of f_s is negligible if $a_s R_c + b_s$ is of order $\mathcal{O}(\epsilon)$ and also results in the same stability/instability properties numerically; see section 5.2. If $a_s R_c + b_s$ is of order $\mathcal{O}(1)$, then the adaptation is not negligible, but the numerical results in section 5.2 illustrate that we obtain the same stability/instability results for f_s^ϵ and f_s.

Remark 4.2. Note that the modeling assumptions in Assumptions 3.1 and 4.1 can be applied to linear repulsive and attractive force coefficients f_R^ϵ and f_A^ϵ as in (4.1), where the total force of the form (2.6) consists of repulsion and attraction forces. That is, for $\epsilon > 0$ we define

(4.2)

$$f_R^\epsilon(|d|) := \begin{cases} a_R|d| + b_R, & |d| \in [0, R_c - \epsilon], \\ (2b_R + 2R_c a_R - a_R\epsilon)\frac{(|d|-R_c)^3}{\epsilon^3} + (3b_R + 3R_c a_R - 2a_R\epsilon)\frac{(|d|-R_c)^2}{\epsilon^2}, & |d| \in (R_c - \epsilon, R_c), \\ 0, & |d| \geq R_c, \end{cases}$$

$$f_A^\epsilon(|d|) := \begin{cases} a_A|d| + b_A, & |d| \in [0, R_c - \epsilon], \\ (2b_A + 2R_c a_A - a_A\epsilon)\frac{(|d|-R_c)^3}{\epsilon^3} + (3b_A + 3R_c a_A - 2a_A\epsilon)\frac{(|d|-R_c)^2}{\epsilon^2}, & |d| \in (R_c - \epsilon, R_c), \\ 0, & |d| \geq R_c, \end{cases}$$

for constants a_A, a_R, b_A, b_R and we require

$$f_R^\epsilon \geq 0 \quad \text{and} \quad f_A^\epsilon \leq 0$$

for all $\epsilon > 0$ with $\epsilon \ll R_c$, implying

$$a_R s + b_R \geq 0 \quad \text{and} \quad a_A s + b_A \leq 0 \quad \text{for} \quad s \in [0, R_c], \tag{4.3}$$

and, in particular,

$$b_R > 0 \quad \text{and} \quad b_A < 0. \tag{4.4}$$

For realistic interaction force coefficients f_R^ϵ and f_A^ϵ we assume that their absolute values decrease as the distance between the particles increases, implying

$$a_R < 0 \quad \text{and} \quad a_A > 0 \tag{4.5}$$

by the definition of f_R^ϵ and f_A^ϵ in (4.2) and by the condition for b_R and b_A in (4.4). Combining the assumptions on a_A, a_R in (4.5) and b_A, b_R in (4.4), condition (4.3) reduces to

$$a_R R_c + b_R \geq 0 \quad \text{and} \quad a_A R_c + b_A \leq 0.$$

Further we assume that $f_A^\epsilon + f_R^\epsilon$ is short-range repulsive, long-range attractive for any $\epsilon > 0$ with $\epsilon \ll R_c$, i.e.,

$$(f_A^\epsilon + f_R^\epsilon)(0) = b_A + b_R > 0, \qquad (f_A^\epsilon + f_R^\epsilon)(R_c - \epsilon) = (a_A + a_R)(R_c - \epsilon) + b_A + b_R < 0$$

for all $0 < \epsilon \ll R_c$ implying

$$b_A + b_R > 0 \quad \text{and} \quad a_A + a_R < 0. \tag{4.6}$$

For any $\epsilon > 0$, the force coefficient $\chi f_A^\epsilon + f_R^\epsilon$ is purely repulsive along s on $[0, R_c - \epsilon]$ if $\chi \in [0, 1]$ is sufficiently small since f_R^ϵ is repulsive. Note that (4.6) implies

$$\chi a_A + a_R < 0, \quad \chi b_A + b_R > 0 \quad \text{for all} \quad \chi \in [0, 1]$$

by the positivity of b_R and by the negativity of a_R in (4.4) and (4.5), respectively. Since

$$f_l^\epsilon(|d|) = f_A^\epsilon(|d|) + f_R^\epsilon(|d|) = (a_A + a_R)\,|d| + b_A + b_R$$

and

$$f_s^\epsilon(|d|) = \chi f_A^\epsilon(|d|) + f_R^\epsilon(|d|) = (\chi a_A + a_R)\,|d| + \chi b_A + b_R$$

for $|d| \in [0, R_c - \epsilon]$, we have

$$a_l = a_A + a_R < 0, \quad a_s = \chi a_A + a_R < 0, \quad b_l = b_A + b_R > 0, \quad b_s = \chi b_A + b_R > 0$$

as in Assumption 4.1.

For investigating the stability of the straight line for any $N \in \mathbb{N}$, we consider the real parts of the eigenvalues in (3.13), i.e.,

$$\Re(\lambda_1(m)) = 2\int_0^{R_c} f_l^\epsilon(s)\,(1 - \cos(-2\pi m s))\,\mathrm{d}s,$$
$$\Re(\lambda_2(m)) = 2\int_0^{R_c} \left(f_s^\epsilon(s) + s(f_s^\epsilon)'(s)\right)(1 - \cos(-2\pi m s))\,\mathrm{d}s.$$

Note that the coefficient functions of the integrands in the definition of the eigenvalues are given by

$$f_l^\epsilon(s) = a_l s + b_l, \quad f_s^\epsilon(s) + s(f_s^\epsilon)'(s) = 2a_s s + b_s$$

for $s \in [0, R_c - \epsilon]$ with $a_l, a_s < 0,\ b_l, b_s > 0$, and

$$f_l^\epsilon(s) = (2b_l + 2R_c a_l - a_l\epsilon)\frac{(s-R_c)^3}{\epsilon^3} + (3b_l + 3R_c a_l - 2a_l\epsilon)\frac{(s-R_c)^2}{\epsilon^2},$$

$$\begin{aligned} f_s^\epsilon(s) + s(f_s^\epsilon)'(s) = {} & (2b_s + 2R_c a_s - a_s\epsilon)\frac{(s-R_c)^3}{\epsilon^3} + (3b_s + 3R_c a_s - 2a_s\epsilon)\frac{(s-R_c)^2}{\epsilon^2} \\ & + 3(2b_s + 2R_c a_s - a_s\epsilon)\frac{s(s-R_c)^2}{\epsilon^3} + 2(3b_s + 3R_c a_s - 2a_s\epsilon)\frac{s\,(s-R_c)}{\epsilon^2} \end{aligned}$$

for $s \in [R_c - \epsilon, R_c]$ by Assumption 4.1. Since $f_l^\epsilon(s)$ and $f_s^\epsilon(s) + s(f_s^\epsilon)'(s)$ are bounded on $[R_c - \epsilon, R_c]$, we obtain

(4.7)

$$\begin{aligned} \Re(\lambda_1(m)) &= 2\int_0^{R_c-\epsilon} (a_l s + b_l)\,(1 - \cos(-2\pi m s))\,\mathrm{d}s + \mathcal{O}(\epsilon), \\ \Re(\lambda_2(m)) &= 2\int_0^{R_c-\epsilon} (2a_s s + b_s)\,(1 - \cos(-2\pi m s))\,\mathrm{d}s \\ &\quad + \frac{12(b_s + R_c a_s)}{\epsilon}\int_{R_c-\epsilon}^{R_c} \left(\frac{s(s-R_c)^2}{\epsilon^2} + \frac{s\,(s-R_c)}{\epsilon}\right)(1 - \cos(-2\pi m s))\,\mathrm{d}s + \mathcal{O}(\epsilon). \end{aligned}$$

Note that $s(f_s^\epsilon)'$ is of order $\mathcal{O}(1/\epsilon)$ on $[R_c - \epsilon, R_c]$ and hence the integral over $[R_c - \epsilon, R_c]$ also contributes to the leading order term for $\Re(\lambda_2(m))$. Here, $f_l^\epsilon(s)$ and $f_s^\epsilon(s) + s(f_s^\epsilon)'(s)$ are linear functions on $[0, R_c - \epsilon]$ of the form $f|_{[0,R_c-\epsilon]} \to \mathbb{R}, s \mapsto as + b$ for constants $a < 0$ and $b > 0$. In particular, $\Re(\lambda_1)$ and the first term in $\Re(\lambda_2)$ are of the form

$$2\int_0^{R_c-\epsilon} (a_k s + b_k)\,(1 - \cos(2\pi m s))\,\mathrm{d}s, \tag{4.8}$$

where

$$a_1 = a_l, \quad a_2 = 2a_s, \quad b_1 = b_l, \quad b_2 = b_s. \tag{4.9}$$

For ease of notation we drop the indices of a_k and b_k in the following. Note that

$$\begin{aligned} &\int_0^{R_c-\epsilon} (as + b)\,(1 - \cos(2\pi m s))\,\mathrm{d}s \\ &= \frac{2\pi m\,(\pi m(R_c - \epsilon)\,(a(R_c - \epsilon) + 2b) - (a(R_c - \epsilon) + b)\sin(2\pi m(R_c - \epsilon)))}{4\pi^2 m^2} \\ &\quad + \frac{a - a\cos(2\pi m(R_c - \epsilon))}{4\pi^2 m^2}. \end{aligned} \tag{4.10}$$

In the limit $m \to \infty$, all terms in the second line of (4.10) vanish except for the first term. Since $R_c > 0$, we require

$$a \le -b\frac{2}{R_c - \epsilon}$$

for high wave number stability for any $\epsilon > 0$ with $\epsilon \ll R_c$. In particular, this condition is consistent with the necessary condition for high wave number stability in Proposition 3.5 for arbitrary force coefficients f_s^ϵ and f_l^ϵ satisfying Assumption 3.1. In the limit $\epsilon \to 0$, it reduces to

$$a \leq -b\frac{2}{R_c}. \tag{4.11}$$

Since $R_c \in (0, 0.5]$ and $b > 0$, (4.11) implies that $a < 0$ is necessary for high wave number stability. Hence, we can assume

$$a < 0 \quad \text{and} \quad b > 0$$

in the following.

Lemma 4.3. *Let $b > 0$ and $R_c \in (0, 0.5]$. For $\epsilon > 0$, set*

$$\begin{aligned} g_\epsilon(m) &:= 2\pi m\left(\pi m(R_c-\epsilon)^2 - (R_c-\epsilon)\sin(2\pi m(R_c-\epsilon))\right) + 1 - \cos(2\pi m(R_c-\epsilon)),\\ h_\epsilon(m) &:= 2\pi m\left(2\pi m(R_c-\epsilon) - \sin(2\pi m(R_c-\epsilon))\right). \end{aligned} \tag{4.12}$$

Then,

$$\int_0^{R_c-\epsilon} (as+b)\left(1-\cos\left(2\pi m s\right)\right) \mathrm{d}s \leq 0 \tag{4.13}$$

is satisfied for all $m \in \mathbb{N}$ and all $\epsilon > 0$ with $\epsilon \ll R_c$ if and only if $a \leq a_0$ with

$$a_0 := -b \max_{m\in\mathbb{N}} \frac{h_\epsilon(m)}{g_\epsilon(m)} \leq -\frac{2b}{R_c} \leq 0. \tag{4.14}$$

Proof. Note that the numerator of (4.10) is of the form $ag_\epsilon(m) + bh_\epsilon(m)$ for functions g_ϵ and h_ϵ, defined in (4.12). Condition (4.13) is equivalent to

$$a \leq -b\frac{h_\epsilon(m)}{g_\epsilon(m)} \quad \text{for all } m \in \mathbb{N}.$$

Herein, $h_\epsilon(m) \geq 0$ for all $m \geq 0$ since h_ϵ is an increasing function. Further note that

$$\begin{aligned} g_\epsilon'(m) &= 2\pi\left(\pi m(R_c-\epsilon)^2 - (R_c-\epsilon)\sin(2\pi m(R_c-\epsilon))\right)\\ &\quad + 2\pi m\left(\pi(R_c-\epsilon)^2 - 2\pi(R_c-\epsilon)^2\cos(2\pi m(R_c-\epsilon))\right) + 2\pi(R_c-\epsilon)\sin(2\pi m(R_c-\epsilon))\\ &= 4\pi^2 m(R_c-\epsilon)^2\left(1-\cos(2\pi m(R_c-\epsilon))\right) \end{aligned}$$

is nonnegative implying that g_ϵ is an increasing function with $g_\epsilon(0) = 0$. In particular, g_ϵ and h_ϵ are nonnegative functions for all $m \in \mathbb{N}$. Hence, (4.13) is satisfied for all $m \in \mathbb{N}$ if and only if $a < a_0$. Note that

$$\lim_{m\to\infty} \frac{h_\epsilon(m)}{g_\epsilon(m)} = \frac{2}{R_c-\epsilon},$$

implying that

$$\sup_{m\in\mathbb{N}} \frac{h_\epsilon(m)}{g_\epsilon(m)} \in \mathbb{R}$$

by the nonnegativity and continuity of g_ϵ and h_ϵ.

Let $R_c \in (0, 0.5]$ and $\epsilon > 0$. We have

$$\begin{aligned}\max_{m\in\mathbb{N}} \frac{h_\epsilon(m)}{g_\epsilon(m)} &\geq \frac{2\pi m\left(2\pi m(R_c-\epsilon) - \sin(2\pi m(R_c-\epsilon))\right)}{2\pi m\left(\pi m(R_c-\epsilon)^2 - (R_c-\epsilon)\sin(2\pi m(R_c-\epsilon))\right)+2} \\ &= \frac{2}{R_c-\epsilon}\left(1 + \frac{\pi m \sin(2\pi m(R_c-\epsilon)) - \frac{2}{R_c-\epsilon}}{2\pi m\left(\pi m(R_c-\epsilon) - \sin(2\pi m(R_c-\epsilon))\right) + \frac{2}{R_c-\epsilon}}\right)\end{aligned}$$

for all $m \in \mathbb{N}$. Since $R_c - \epsilon \in (0, 0.5)$ there exists $m \in \mathbb{N}$ such that $\pi m \sin(2\pi m(R_c-\epsilon)) - \frac{2}{R_c-\epsilon} > 0$ and hence

$$\max_{m\in\mathbb{N}} \frac{h_\epsilon(m)}{g_\epsilon(m)} > \frac{2}{R_c-\epsilon} > \frac{2}{R_c}$$

for $\epsilon > 0$ with $\epsilon \ll R_c$. For $R_c \in (0, 0.5)$, we obtain

$$\lim_{\epsilon\to 0}\max_{m\in\mathbb{N}} \frac{h_\epsilon(m)}{g_\epsilon(m)} > \frac{2}{R_c}.$$

For $R_c = 0.5$, we have

$$\lim_{\epsilon\to 0} \frac{h_\epsilon(m)}{g_\epsilon(m)} = \begin{cases} \frac{2}{R_c}, & m \text{ even}, \\ \frac{4\pi^2 R_c}{2\pi^2 R_c^2 + \frac{2}{m^2}} < \frac{2}{R_c}, & m \text{ odd}, \end{cases}$$

implying that

$$\lim_{\epsilon\to 0}\max_{m\in\mathbb{N}} \frac{h_\epsilon(m)}{g_\epsilon(m)} = \frac{2}{R_c}.$$

Hence, $a \leq a_0$ is equivalent to the necessary condition (4.11) for high wave number stability for $R_c = 0.5$. ∎

Remark 4.4. For the stability of line patterns with force coefficients $f_s^\epsilon, f_l^\epsilon$ of the form (4.1), we require $\Re(\lambda_k(m)) \leq 0$ for $k = 1, 2$ for the real parts of the eigenvalues $\Re(\lambda_k(m))$, $k = 1, 2$, in (4.7). Note that the nonnegativity of the leading order term of $\Re(\lambda_1)$ which is of the form (4.8) is equivalent to condition (4.13) in Lemma 4.3. Similarly, the nonnegativity of the first term in (4.7) which is also of the form (4.8) is equivalent to condition (4.13) in Lemma 4.3.

From the proof of Lemma 4.3 it follows that

$$\frac{2}{R_c} \leq \max_{m\in\mathbb{N}} \frac{h_\epsilon(m)}{g_\epsilon(m)}. \tag{4.15}$$

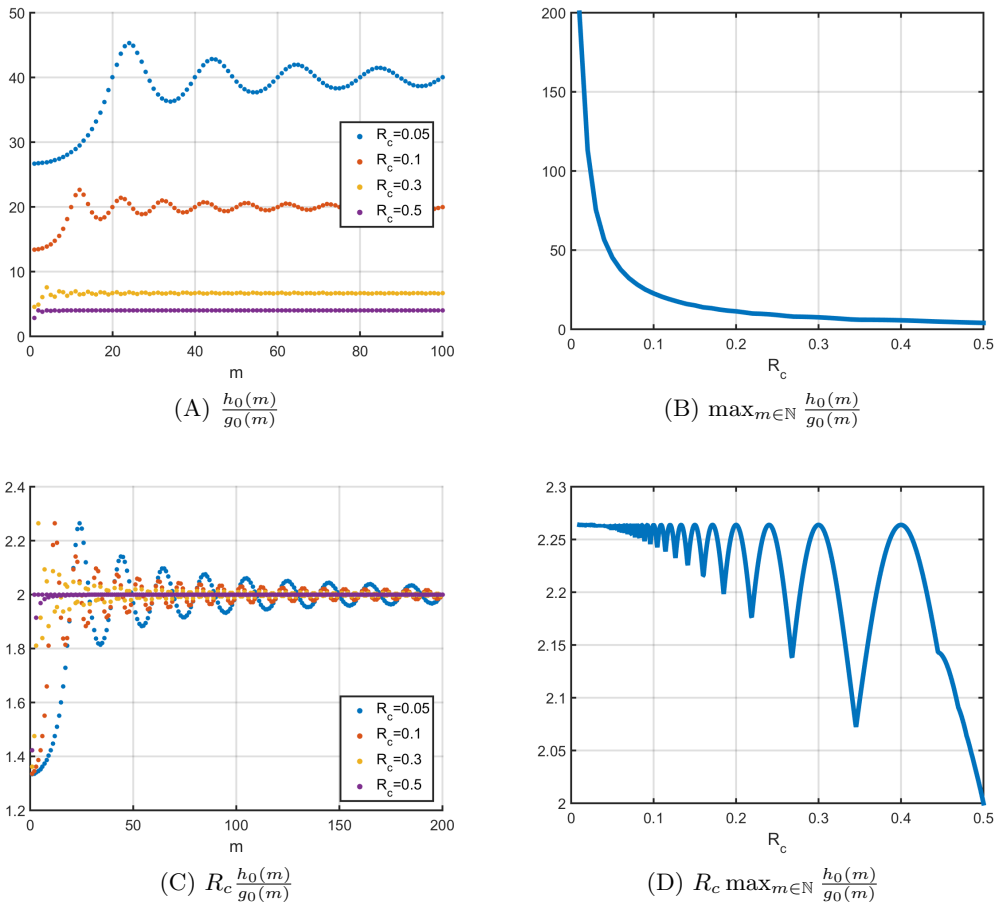

(A) $\frac{h_0(m)}{g_0(m)}$ (B) $\max_{m\in\mathbb{N}} \frac{h_0(m)}{g_0(m)}$

(C) $R_c \frac{h_0(m)}{g_0(m)}$ (D) $R_c \max_{m\in\mathbb{N}} \frac{h_0(m)}{g_0(m)}$

Figure 2. *Scaling factor of a_0 in (4.14) as a function of R_c where g_0, h_0 are defined in (4.12).*

The inequality in (4.15) is strict for $R_c - \epsilon \in (0, 0.5)$, i.e., a necessary condition for (4.13) to hold for $R_c - \epsilon \in (0, 0.5)$ is given by

$$a < -\frac{2b}{R_c}.$$

For $R_c = 0.5$ and $\epsilon \to 0$, condition (4.13) holds for any $a < 0$ satisfying the necessary condition (4.11) for high wave number stability. If the necessary condition (4.11) for high wave number stability is satisfied with equality, i.e., $a = -\frac{2b}{R_c}$, the leading order term of the left-hand side of (4.7) vanishes for $\epsilon \to 0$ in the high wave limit and lower order terms have to be considered.

In Figure 2, we investigate the scaling factor of a_0, defined in (4.14), numerically. In Figure 2(A) the quotient h_0/g_0 is shown as a function of $m \in \mathbb{N}$ for different values of the cutoff radius R_c. Note that for smaller values of R_c, the maximum of h_0/g_0 gets larger as shown in Figure 2(B). In Figures 2(C) and 2(D) we consider the quotient h_0/g_0 scaled by R_c. Figure 2(C) shows that $R_c h_0/g_0 \to 2$ as $m \to \infty$, independently of the value of R_c, and that

the maximum of $R_c h_0/g_0$ is obtained for smaller values of $m \in \mathbb{N}$ in general. The value of

$$R_c \max_{m\in\mathbb{N}} \frac{h_0(m)}{g_0(m)}$$

is shown in Figure 2(D) as a function of R_c. In particular, the scaled maximum is larger than 2 if and only if $R_c \in (0, 0.5)$ and is equal to 2 for $R_c = 0.5$. Hence, this numerical investigation is consistent with the results in Lemma 4.3.

Applying Lemma 4.3 to the specific form of the stability conditions for a single straight vertical line leads to the following stability results for the linear force coefficients (4.1).

Proposition 4.5. *For $R_c \in (0, 0.5)$, the single straight vertical line is an unstable steady state of (2.9) for any $N \in \mathbb{N}$ sufficiently large and in the continuum limit $N \to \infty$, where the forces are of the form (2.7) for any linear coefficient functions $f_s^\epsilon, f_l^\epsilon$ with $0 < \epsilon \ll R_c$ such that Assumption 4.1 is satisfied. In particular, the single straight vertical line is an unstable steady state for force coefficients $f_s^\epsilon, f_l^\epsilon$ for $R_c \in (0, 0.5)$ in the limit $\epsilon \to 0$.*

Proof. Note that the leading order term of $\Re(\lambda_1(m))$ and the first term of $\Re(\lambda_2(m))$ in (4.7) are of the form (4.8) with parameters (4.9). For stability we require $\Re(\lambda_k) \le 0$ for $k = 1, 2$.

Let us consider the nonnegativity of $\Re(\lambda_2(m))$ in (4.7) first. Note that the second leading order term of $\Re(\lambda_2(m))$ in (4.7) can be rewritten as

$$\begin{aligned} &12(b_s + R_c a_s) \int_{-1}^{0} ((\epsilon s + R_c)s^2 + (\epsilon s + R_c)s)\,(1 - \cos(2\pi m(\epsilon s + R_c)))\,\mathrm{d}s \\ &= -2(b_s + R_c a_s) R_c\,(1 - \cos(2\pi m R_c)) + \mathcal{O}(\epsilon). \end{aligned} \tag{4.16}$$

Hence, $\Re(\lambda_2(m))$ is of the form

$$\Re(\lambda_2(m)) = \frac{2}{4\pi^2 m^2}(2a_s g_0(m) + b_s h_0(m)) - 2(b_s + R_c a_s) R_c\,(1 - \cos(2\pi m R_c)) + \mathcal{O}(\epsilon)$$

by (4.10), where g_0, h_0 are defined in (4.12). For the nonnegativity of the leading order term of $\Re(\lambda_2(m))$ we require

$$a_s\left(\frac{2g_0(m)}{4\pi^2 m^2} - R_c^2\,(1 - \cos(2\pi m R_c))\right) + b_s\left(\frac{h_0(m)}{4\pi^2 m^2} - R_c\,(1 - \cos(2\pi m R_c))\right) \le 0,$$

which can be rewritten as

$$a_s \tilde{g}_0(m) + b_s \tilde{h}_0(m) \le 0,$$

where

$$\begin{aligned} \tilde{g}_0(m) &:= 2\pi m\left(2\pi m R_c^2 \cos(2\pi m R_c) - 2R_c \sin(2\pi m R_c)\right) + 2 - 2\cos(2\pi m R_c), \\ \tilde{h}_0(m) &:= 2\pi m\,(2\pi m R_c \cos(2\pi m R_c) - \sin(2\pi m R_c))\,. \end{aligned}$$

For m sufficiently large, we have

$$a_s \tilde{g}_0(m) + b_s \tilde{h}_0(m) = 4\pi^2 m^2 R_c^2 \cos(2\pi m R_c) a_s + 4\pi^2 m^2 R_c \cos(2\pi m R_c) b_s + \mathcal{O}(m)$$

and by only considering the leading order term we obtain the condition

$$R_c \cos(2\pi m R_c) a_s + \cos(2\pi m R_c) b_s \leq 0.$$

Note that there exist infinitely many $m \in \mathbb{N}$ such that $\cos(2\pi m R_c) > 0$ and such that $\cos(2\pi m R_c) < 0$, independently of the choice of $R_c \in (0, 0.5)$. Hence, we can conclude $a_s R_c + b_s = 0$. In this case, the second leading order term of $\Re(\lambda_2(m))$ vanishes by (4.16) and thus, it is sufficient to consider $\Re(\lambda_1(m))$ and the first term of $\Re(\lambda_2(m))$ in (4.7). Applying Lemma 4.3 together with Remark 4.4 for $R_c \in (0, 0.5)$ to the linear force coefficients $f_l^\epsilon, f_s^\epsilon$ in (4.1) results in the stability conditions

$$a_l < -\frac{2b_l}{R_c} \quad \text{and} \quad a_s < -\frac{b_s}{R_c} \tag{4.17}$$

for any $\epsilon > 0$ which are necessary for the nonnegativity of $\Re(\lambda_1(m))$ and the (first) leading order term of $\Re(\lambda_2(m))$. Hence, the single straight vertical line is unstable for $R_c \in (0, 0.5)$ and $0 < \epsilon \ll R_c$, both in the continuum limit $N \to \infty$ and for any $N \in \mathbb{N}$ sufficiently large. Similarly, we obtain instability of straight vertical line patterns for force coefficients $f_s^\epsilon, f_l^\epsilon$ for $R_c \in (0, 0.5)$ in the limit $\epsilon \to 0$. ∎

Remark 4.6. For $R_c = 0.5$, we cannot conclude stability/instability of the straight vertical line for the linear force coefficients in (4.1) with $a_s = -\frac{b_s}{R_c}$, while we can conclude instability for $a_s \neq -\frac{b_s}{R_c}$. To see this, note that for $R_c = 0.5$ the calculations in the proof of Proposition 4.5 imply $a_s = -\frac{b_s}{R_c}$ as a necessary condition for stability; from Lemma 4.3 we obtain

$$a_l \leq -\frac{2b_l}{R_c} \quad \text{and} \quad a_s \leq -\frac{b_s}{R_c},$$

and together with the condition that f_s^ϵ is purely repulsive we get the necessary conditions

$$a_l \leq -\frac{2b_l}{R_c} \quad \text{and} \quad a_s = -\frac{b_s}{R_c} \tag{4.18}$$

for the stability of the straight vertical line. Note that the conditions (4.18) are consistent with each other since $a_l, a_s < 0$ and $b_l, b_s > 0$ by Assumption 4.1 and it is possible to choose the parameters a_l, a_s, b_l, b_s in such a way that both (4.18) and the assumptions on the force coefficients $f_s^\epsilon, f_l^\epsilon$ in Assumption 4.1 are satisfied. In this case, we have

$$f_s^\epsilon(s) + s(f_s^\epsilon)'(s) = a_s(2s - 0.5)$$

for $s \in [0, 0.5 - \epsilon]$ with $a_s < 0$ and

$$f_s^\epsilon(s) + s(f_s^\epsilon)'(s) = -a_s \frac{(s - R_c)^3}{\epsilon^2} - 2a_s \frac{(s - R_c)^2}{\epsilon} - 3a_s \frac{s(s - R_c)^2}{\epsilon^2} - 4a_s \frac{s\,(s - R_c)}{\epsilon}$$

for $s \in [0.5 - \epsilon, 0.5]$ by Assumption 4.1. Clearly, the leading order term of $\Re(\lambda_2(m))$ vanishes in the high wave limit $m \to \infty$ and lower order terms in ϵ have to be considered. An easy computation reveals that

$$\lim_{m \to \infty} \Re(\lambda_2(m)) = 2 \int_0^{0.5} f_s^\epsilon(s) + s(f_s^\epsilon)'(s) = 0 \tag{4.19}$$

for any $\epsilon > 0$ and as $\epsilon \to 0$. Further note that using (4.19), $\Re(\lambda_2(m))$ reduces to

$$\Re(\lambda_2(m)) = -2\int_0^{0.5} \left(f_s^\epsilon(s) + s(f_s^\epsilon)'(s)\right)\cos(2\pi m s)\,\mathrm{d}s.$$

We obtain

$$\int_0^{0.5-\epsilon} a_s(2s-0.5)\cos(2\pi m s)\,\mathrm{d}s = \begin{cases} -0.5a_s\epsilon + a_s\epsilon^2 + \mathcal{O}(\epsilon^3), & m \in 2\mathbb{N}, \\ -\frac{a_s}{\pi^2 m^2} + 0.5a_s\epsilon - a_s\epsilon^2 + \mathcal{O}(\epsilon^3), & m \in 2\mathbb{N}+1, \end{cases}$$

$$-a_s\int_{0.5-\epsilon}^{0.5}\left(\frac{(s-R_c)^3}{\epsilon^2} + 2\frac{(s-R_c)^2}{\epsilon}\right)\cos(2\pi m s)\,\mathrm{d}s = \begin{cases} -\frac{5}{12}a_s\epsilon^2 + \mathcal{O}(\epsilon^3), & m \in 2\mathbb{N}, \\ \frac{5}{12}a_s\epsilon^2 + \mathcal{O}(\epsilon^3), & m \in 2\mathbb{N}+1, \end{cases}$$

$$-3a_s\int_{0.5-\epsilon}^{0.5}\frac{s\,(s-R_c)^2}{\epsilon^2}\cos(2\pi m s)\,\mathrm{d}s = \begin{cases} -0.5a_s\epsilon + \frac{3}{4}a_s\epsilon^2 + \mathcal{O}(\epsilon^3), & m \in 2\mathbb{N}, \\ 0.5a_s\epsilon - \frac{3}{4}a_s\epsilon^2 + \mathcal{O}(\epsilon^3), & m \in 2\mathbb{N}+1, \end{cases}$$

and

$$-4a_s\int_{0.5-\epsilon}^{0.5}\frac{s\,(s-R_c)}{\epsilon}\cos(2\pi m s)\,\mathrm{d}s = \begin{cases} a_s\epsilon - \frac{4}{3}a_s\epsilon^2 + \mathcal{O}(\epsilon^3), & m \in 2\mathbb{N}, \\ -a_s\epsilon + \frac{4}{3}a_s\epsilon^2 + \mathcal{O}(\epsilon^3), & m \in 2\mathbb{N}+1, \end{cases}$$

implying that

$$\int_0^{0.5}\left(f_s^\epsilon(s) + s(f_s^\epsilon)'(s)\right)\cos(2\pi m s)\,\mathrm{d}s = \begin{cases} \mathcal{O}(\epsilon^3), & m \in 2\mathbb{N}, \\ -\frac{a_s}{\pi^2 m^2} + \mathcal{O}(\epsilon^3), & m \in 2\mathbb{N}+1. \end{cases}$$

Since the real part of the largest eigenvalue $\Re(\lambda_2(m))$ is zero in the high wave number limit and it vanishes in the limit $\epsilon \to 0$ for any $m \in \mathbb{N}$, we cannot conclude stability/instability of the straight vertical line for $R_c = 0.5$ and $\epsilon > 0$ or $\epsilon \to 0$ in the continuum limit $N \to \infty$ or any $N \in \mathbb{N}$ sufficiently large. However, the numerical results in section 5.2 suggest instability for $\epsilon > 0$ and in the limit $\epsilon \to 0$.

Since we have the relations $f_l^\epsilon = f_A^\epsilon + f_R^\epsilon$ and $f_s^\epsilon = \chi f_A^\epsilon + f_R^\epsilon$ between the force coefficients $f_l^\epsilon, f_s^\epsilon$ in the general force formulation (2.7) and the total force (2.6) in the Kücken–Champod model with repulsive and attractive force coefficients f_R^ϵ and f_A^ϵ, respectively, we have

$$a_l = a_A + a_R, \quad a_s = \chi a_A + a_R, \quad b_l = b_A + b_R, \quad b_s = \chi b_A + b_R.$$

Hence, Proposition 4.5 leads to a similar statement for the forces in the Kücken–Champod model.

Corollary 4.7. *For $R_c \in (0, 0.5)$ the single straight vertical line is an unstable steady state of (2.9) for any $N \in \mathbb{N}$ sufficiently large and for the continuum limit $N \to \infty$, where the forces*

are of the form (2.7) *for any choice of parameters in the definition of the linear coefficient functions* $f_R^\epsilon, f_A^\epsilon$ *in* (4.2) *with* $0 < \epsilon \ll R_c$ *or* $\epsilon \to 0$. *For* $R_c = 0.5$, *the condition*

$$a_A + a_R \leq -\frac{2\,(b_A + b_R)}{R_c} \quad \text{and} \quad \chi a_A + a_R = -\frac{\chi b_A + b_R}{R_c}$$

in addition to the assumptions on a_A, a_R, b_A, b_R *in Remark* 4.2 *is necessary for the stability of the single straight vertical line for force coefficients* $f_R^\epsilon, f_A^\epsilon$, *where* $0 < \epsilon \ll R_c$ *or* $\epsilon \to 0$. *This does not guarantee the stability/instability of the straight vertical line for force coefficients* $f_R^\epsilon, f_A^\epsilon$ *with* $0 < \epsilon \ll R_c$ *or* $\epsilon \to 0$ *for* $R_c = 0.5$ *and* $N \in \mathbb{N}$ *sufficiently large or in the continuum limit* $N \to \infty$.

4.2. Algebraically decaying force coefficients. Since the straight vertical line is unstable for $N \in \mathbb{N}$ sufficiently large and for $N \to \infty$ for the differentiable force coefficient f_s^ϵ, defined in (4.1) along s, which is linear on $[0, R_c - \epsilon]$ for $R_c \in (0, 0.5)$ and $\epsilon > 0$, we consider faster decaying force coefficients along s in the following. In this section we consider

$$f_s(|d|) = \frac{c}{(1 + a|d|)^b}$$

for $a > 0$, $b > 0$, and $c > 0$. To obtain a differentiable force coefficient f_s^ϵ on $(0, \infty)$ we consider the modification in (2.10), i.e.,

$$f_s^\epsilon(|d|) = \begin{cases} \frac{c}{(1+a|d|)^b}, & |d| \in [0, R_c - \epsilon], \\ -\frac{abc}{(1+a(R_c-\epsilon))^{b+1}} \left(\frac{(|d|-R_c)^3}{\epsilon^2} + \frac{(|d|-R_c)^2}{\epsilon} \right) & \\ \quad + \frac{c}{(1+a(R_c-\epsilon))^b} \left(2\frac{(|d|-R_c)^3}{\epsilon^3} + 3\frac{(|d|-R_c)^2}{\epsilon^2} \right), & |d| \in (R_c - \epsilon, R_c), \\ 0, & |d| \geq R_c, \end{cases}$$

where $R_c \in (0, 0.5]$. Note that for this algebraically decaying force coefficient f_s^ϵ, the necessary condition $f_s^\epsilon(R_c) = 0$ in (3.17) for high wave number stability of a straight vertical line is satisfied. To guarantee that the term $a|d|$ for $|d| \in [0, R_c]$ dominates the denominator and to avoid too large jumps we require $a \gg 1$ additionally. The assumption $a \gg 1$ also guarantees that $f_s^\epsilon(R_c - \epsilon) \ll 1$. In this case, differences between the adaptation f_s^ϵ and the algebraically decaying force coefficient f_s, and their derivatives $(f_s^\epsilon)'$ and f_s', are small. Without loss of generality we can assume that $c = 1$ since this positive multiplicative constant leads to a rescaled stability condition but is not relevant for change of sign of the eigenvalues. Hence, we consider the algebraically decaying force coefficient

$$f_s^\epsilon(|d|) = \begin{cases} \frac{1}{(1+a|d|)^b}, & |d| \in [0, R_c - \epsilon], \\ -\frac{ab}{(1+a(R_c-\epsilon))^{b+1}} \left(\frac{(|d|-R_c)^3}{\epsilon^2} + \frac{(|d|-R_c)^2}{\epsilon} \right) & \\ \quad + \frac{1}{(1+a(R_c-\epsilon))^b} \left(2\frac{(|d|-R_c)^3}{\epsilon^3} + 3\frac{(|d|-R_c)^2}{\epsilon^2} \right), & |d| \in (R_c - \epsilon, R_c), \\ 0, & |d| \geq R_c \end{cases} \tag{4.20}$$

in the following.

Proposition 4.8. *For the single straight vertical line to be a stable steady state of (2.9) with forces of the form (2.1) for any $n \in \mathbb{N}$ sufficiently large and for the continuum limit $N \to \infty$ with algebraically decaying force coefficients f_s^ϵ of the form (4.20) it is necessary that*

$$b > 1 \quad \text{and} \quad \frac{2}{a(b-1)} < R_c.$$

Proof. Because of the definition of the eigenvalues (3.13) we consider

$$\begin{aligned} &\int_0^{R_c} \left(f_s^\epsilon(s) + s(f_s^\epsilon)'(s)\right)\left(1-\cos\left(-2\pi m s\right)\right) \mathrm{d}s \\ &= \int_0^{R_c-\epsilon} \frac{1}{(1+as)^{b+1}}\left(1+as(1-b)\right)\left(1-\cos\left(-2\pi m s\right)\right) \mathrm{d}s + \mathcal{O}(\epsilon). \end{aligned} \tag{4.21}$$

The linear function $1+as(1-b)$ is positive for $s \in (0, s_0)$ and negative for $s \in (s_0, R_c - \epsilon)$ for all $\epsilon > 0$, where

$$s_0 = \frac{1}{a(b-1)} \in (0, R_c),$$

implying $b > 1$. Note that the integral on the right-hand side of (4.21) can be rewritten as

$$\int_0^{R_c-\epsilon} g(s)\,\mathrm{d}s = \int_0^{s_0} g(s)\,\mathrm{d}s + \int_{s_0}^{R_c-\epsilon} g(s)\,\mathrm{d}s$$

for any $\epsilon > 0$, where

$$g(s) = \frac{1}{(1+as)^{b+1}}\left(1+as(1-b)\right)\left(1-\cos\left(-2\pi m s\right)\right)$$

is nonnegative on $[0, s_0]$ and not positive on $[s_0, R_c - \epsilon]$ for any $\epsilon > 0$ by the definition of s_0 and the fact that $1 - \cos(-2\pi m s) \in (0, 2)$. Setting

$$h(s) = \frac{1}{(1+as)^{b+1}},$$

note that $h(R_c) < h(s_0) < h(0) = 1$. A lower bound of the integral can be obtained by estimating $h(s)$ on $[0, s_0]$ by $h(s_0)$ due to the nonnegativity of the integrand, and since the integrand changes sign at s_0 the factor $h(s)$ can be replaced by its maximum on $[s_0, R_c - \epsilon]$ for $\epsilon > 0$, i.e., by $h(s_0)$. Hence, a lower bound of the integral in (4.21) is given by

$$\begin{aligned} &\frac{1}{(1+as_0)^{b+1}} \int_0^{R_c-\epsilon} \left(1+as(1-b)\right)\left(1-\cos\left(-2\pi m s\right)\right) \mathrm{d}s + \mathcal{O}(\epsilon) \\ &= \frac{1}{(1+as_0)^{b+1}} \left(\frac{2\pi m\left(\pi m(R_c-\epsilon)\left(p(R_c-\epsilon)+2q\right) - \left(p(R_c-\epsilon)+q\right)\sin\left(2\pi m(R_c-\epsilon)\right)\right)}{4\pi^2 m^2} \right. \\ &\qquad \left. + \frac{p - p\cos\left(2\pi m(R_c-\epsilon)\right)}{4\pi^2 m^2} \right) + \mathcal{O}(\epsilon) \end{aligned}$$

with $p = a(1-b)$ and $q = 1$, where the explicit computation is analogous to the discussion of the linear force coefficients in (4.10). For large values of m the first term of the above right-hand side dominates and we require

$$pR_c + 2q = a(1-b)R_c + 2 < 0$$

for all $\epsilon > 0$. This concludes the proof. ∎

In the following, we can restrict ourselves to algebraically decaying force coefficients (4.20) with $a > 0,\ b > 1$ due to Proposition 4.8. We show that the straight vertical line (3.3) is an unstable steady state for any $N \in \mathbb{N}$ sufficiently large and in the continuum limit $N \to \infty$ in this case. Due to the definition of the eigenvalues in (3.13) in Theorem 3.3 it is sufficient to show that there exists $m \in \mathbb{N}$ such that

$$0 < \int_0^{R_c-\epsilon} \left(f_s^\epsilon(s) + s(f_s^\epsilon)'(s)\right)\left(1 - \cos\left(-2\pi m s\right)\right) \mathrm{d}s$$

for all $0 < \epsilon \ll R_c$. This is equivalent to showing that there exists $m \in \mathbb{N}$ such that

$$0 < \lim_{\epsilon \to 0} \int_0^{R_c-\epsilon} \frac{1}{(1+as)^{b+1}} \left(1 + as(1-b)\right)\left(1 - \cos\left(-2\pi m s\right)\right) \mathrm{d}s. \tag{4.22}$$

is satisfied.

Lemma 4.9. *For any $a > 0,\ b > 1$, and $R_c \in (0, 0.5]$ there exists $m \in \mathbb{N}$ such that (4.22) is satisfied.*

Proof. We denote the incomplete gamma function by

$$\Gamma(y, z) = \int_z^\infty s^{y-1} \exp(-s)\, \mathrm{d}s$$

for $y \in \mathbb{R}$ and $z \in \mathbb{C}$. Then the right-hand side of (4.22) can be written as

$$\begin{aligned}
&-\frac{1}{4a\pi m\left(1+aR_c\right)^b}\left(2a\sin(-2\pi m R_c)\right.\\
&+\Re\left[\sin\left(\frac{2\pi m}{a}\right) m^{b+1}\left(c_1\Gamma\left(-b, \frac{2i\pi m}{a}\right) + c_2\Gamma\left(-b, \frac{2i\pi(1+aR_c)m}{a}\right)\right)\right.\\
&+\sin\left(\frac{2\pi m}{a}\right) m^{b}\left(c_3\Gamma\left(1-b, \frac{2i\pi m}{a}\right) + c_4\Gamma\left(1-b, \frac{2i\pi(1+aR_c)m}{a}\right)\right)\\
&+\cos\left(\frac{2\pi m}{a}\right) m^{b+1}\left(c_5\Gamma\left(-b, \frac{2i\pi m}{a}\right) + c_6\Gamma\left(-b, \frac{2i\pi(1+aR_c)m}{a}\right)\right)\\
&+\left.\left.\cos\left(\frac{2\pi m}{a}\right) m^{b}\left(c_7\Gamma\left(1-b, \frac{2i\pi m}{a}\right) + c_8\Gamma\left(1-b, \frac{2i\pi(1+aR_c)m}{a}\right)\right)\right]\right)
\end{aligned}$$

for constants $c_i \in \mathbb{C}, i = 1, \ldots, 8$, depending on a, b, and R_c, but independent of m where not all constants c_i are equal to zero. Note that all incomplete gamma functions above are of the form $\Gamma(-y, iz)$ for $y, z \in \mathbb{R}$ with $y, z > 0$. Integration by parts yields

$$\Gamma(-y, iz) = (iz)^{-y-1}\exp(-iz) + (-y-1)\Gamma(-y-1, iz),$$

where

$$|\Gamma(-y-1,iz)| = \left| \int_{iz}^{\infty} s^{-y-2} \exp(-s)\, \mathrm{d}s \right| \leq |(iz)^{-y-2} \exp(-iz)|.$$

In particular, we have

$$\Gamma(-y,iz) = (iz)^{-y-1} \exp(-iz) \left(1 + \mathcal{O}((iz)^{-1})\right),$$

implying

$$\Re(\Gamma(-y,iz)) = \tilde{c} z^{-y-1} \left(1 + \mathcal{O}(z^{-1})\right),$$

where $\tilde{c} = \Re(i^{-y-1} \exp(-iz)) \in \mathbb{R}$. This leads to the approximation

$$\begin{aligned} &\Re\left[\sin\left(\frac{2\pi m}{a}\right) m^{b+1} \left(c_1 \Gamma\left(-b, \frac{2i\pi m}{a}\right) + c_2 \Gamma\left(-b, \frac{2i\pi(1+aR_c)m}{a}\right)\right)\right. \\ &\quad \left. + \sin\left(\frac{2\pi m}{a}\right) m^{b} \left(c_3 \Gamma\left(1-b, \frac{2i\pi m}{a}\right) + c_4 \Gamma\left(1-b, \frac{2i\pi(1+aR_c)m}{a}\right)\right)\right] \\ &= \tilde{c}_1 \sin\left(\frac{2\pi m}{a}\right) \left(1 + \mathcal{O}(m^{-1})\right) \end{aligned}$$

for some constant $\tilde{c}_1 \in \mathbb{R}$. The other terms of the right-hand side of (4.22) can be rewritten in a similar way, resulting in

$$-\frac{1}{4a\pi m\,(1+aR_c)^b} \left(-2a \sin(2\pi m R_c) + \tilde{c}_1 \sin\left(\frac{2\pi m}{a}\right) + \tilde{c}_2 \cos\left(\frac{2\pi m}{a}\right) + \mathcal{O}(m^{-1})\right)$$

for constants $\tilde{c}_1, \tilde{c}_2 \in \mathbb{R}$, independent of m. Note that there exist infinitely many $m \in \mathbb{N}$ such that $\tilde{c}_1 \sin\left(\frac{2\pi m}{a}\right) + \tilde{c}_2 \cos\left(\frac{2\pi m}{a}\right) > 0$ and such that $\tilde{c}_1 \sin\left(\frac{2\pi m}{a}\right) + \tilde{c}_2 \cos\left(\frac{2\pi m}{a}\right) < 0$. If $R_c = \frac{1}{a}$, the second factor consists of the sum of a sine and a cosine function of the same period length and hence for $R_c \in (0, 0.5]$ given, there exists $m \in \mathbb{N}$ such that the second factor is negative and the leading order term of (4.22) is positive. If the first term in the second factor is of different period length as the second and third summand, there also exists $m \in \mathbb{N}$ such that the second factor is negative. In particular, this implies that there exists an $m \in \mathbb{N}$ such that (4.22) is satisfied. ∎

Corollary 4.10. *For any cutoff radius $R_c \in (0, 0.5]$ the single straight vertical line is an unstable steady state of (2.9) for any $N \in \mathbb{N}$ sufficiently large and for the continuum limit $N \to \infty$ with forces of the form (2.1) with algebraically decaying force coefficients f_s^ϵ of the form (4.20) with $b > 0$ and for any $\epsilon > 0$ or in the limit $\epsilon \to 0$.*

4.3. Exponential force coefficients. In this section we consider exponentially decaying force coefficients along s and short-range repulsive, long-range attractive forces along l such that the necessary condition (3.17) for high wave number stability is satisfied.

To express the force coefficient along l in terms of exponentially decaying functions we consider

(4.23)
$$f_l^\epsilon(|d|) = \begin{cases} c_{l_1}\exp(-e_{l_1}|d|) + c_{l_2}\exp(-e_{l_2}|d|), & |d| \in [0, R_c-\epsilon], \\ \sum_{j=1}^2(-\epsilon c_{l_j}e_{l_j} + 2c_{l_j})\exp(-e_{l_j}(R_c-\epsilon))\frac{(|d|-R_c)^3}{\epsilon^3} & \\ \quad + \sum_{j=1}^2(-\epsilon c_{l_j}e_{l_j} + 3c_{l_j})\exp(-e_{l_j}(R_c-\epsilon))\frac{(|d|-R_c)^2}{\epsilon^2}, & |d| \in (R_c-\epsilon, R_c), \\ 0, & |d| \geq R_c, \end{cases}$$

for parameters $c_{l_1}, c_{l_2}, e_{l_1}$ and e_{l_2} with $e_{l_1} > 0$ and $e_{l_2} > 0$. Note that exponentially decaying functions are either purely repulsive or purely attractive, depending on the sign of the multiplicative parameter. Since we require f_l^ϵ to be short-range repulsive, long-range attractive we consider the sum of two exponentially decaying functions here. Without loss of generality we assume that the first summand in (4.23) is repulsive and the second one is attractive, i.e., $c_{l_1} > 0 > c_{l_2}$. To guarantee that f_l^ϵ is short-range repulsive we require $c_{l_1} > |c_{l_2}|$. For long-range attractive forces we require that the second term decays slower, i.e., $e_{l_1} > e_{l_2}$. These assumptions lead to the parameter choice

(4.24)
$$c_{l_1} > 0 > c_{l_2}, \quad c_{l_1} > |c_{l_2}|, \quad \text{and} \quad e_{l_1} > e_{l_2} > 0.$$

Note that we have

$$\int_0^{R_c} f_l^\epsilon(s)\,(1-\cos(-2\pi m s))\,\mathrm{d}s = \int_0^{R_c-\epsilon} f_l^\epsilon(s)\,(1-\cos(-2\pi m s))\,\mathrm{d}s + \mathcal{O}(\epsilon)$$

due to the boundedness of f_l^ϵ on $[R_c-\epsilon, R_c]$ and hence it is sufficient to consider the integral on $[0, R_c-\epsilon]$ for $\epsilon > 0$ sufficiently small and in the limit $\epsilon \to 0$. Further note that for constants $c, e_l \in \mathbb{R}$ we obtain

$$\int_0^{R_c-\epsilon} c\exp(-e_l s)\,\mathrm{d}s = (1-\exp(-e_l(R_c-\epsilon)))\,\frac{c}{e_l}.$$

Hence, we require

$$(1-\exp(-e_{l_1}(R_c-\epsilon)))\,\frac{c_{l_1}}{e_{l_1}} + (1-\exp(-e_{l_2}(R_c-\epsilon)))\,\frac{c_{l_2}}{e_{l_2}} \leq 0$$

for all $\epsilon > 0$ as in the necessary condition for high wave number stability, implying

$$\frac{c_{l_1}}{e_{l_1}} \leq \frac{|c_{l_2}|}{e_{l_2}}.$$

Since

$$\int_0^{R_c-\epsilon} c_{l_1}\exp(-e_{l_1}s)\,(1-\cos(-2\pi m s))\,\mathrm{d}s > 0,$$
$$\int_0^{R_c-\epsilon} c_{l_2}\exp(-e_{l_2}s)\,(1-\cos(-2\pi m s))\,\mathrm{d}s < 0$$

for all $\epsilon > 0$ and $m \in \mathbb{N}$ the parameters $c_{l_1}, c_{l_2}, e_{l_1}, c_{l_2}$ in (4.24) can clearly be chosen in such a way that

$$\int_0^{R_c-\epsilon} f_l^\epsilon(s)\,(1-\cos(-2\pi m s))\,\mathrm{d}s \le 0 \tag{4.25}$$

is satisfied for all $m \in \mathbb{N}$ and $0 < \epsilon \ll R_c$, where f_l^ϵ is defined in (4.23) with a cutoff radius $R_c \in (0, 0.5]$. Note that the adaptation f_l^ϵ of f_l is not negligible. However, due to the concentration of the particles along a straight vertical axis, this adaptation does not change the overall dynamics.

For the purely repulsive force coefficient f_s^ϵ we may consider a force coefficient of the form

$$f_s^\epsilon \colon \mathbb{R}_+ \to \mathbb{R},$$
$$f_s^\epsilon(|d|) = \begin{cases} c\exp(-e_s|d|), & |d| \in [0, R_c-\epsilon], \\ -ce_s\exp(-e_s(R_c-\epsilon))\left(\frac{(|d|-R_c)^3}{\epsilon^2} + \frac{(|d|-R_c)^2}{\epsilon}\right) & \\ \quad + c\exp(-e_s(R_c-\epsilon))\left(2\frac{(|d|-R_c)^3}{\epsilon^3} + 3\frac{(|d|-R_c)^2}{\epsilon^2}\right), & |d| \in (R_c-\epsilon, R_c), \\ 0, & |d| \ge R_c, \end{cases}$$

by considering (2.10) for exponentially decaying force coefficients. Since

$$\Re(\lambda_2(m)) = 2\int_0^{R_c-\epsilon} \left(f_s^\epsilon(s) + (f_s^\epsilon)'(s)s\right)(1-\cos(-2\pi m s))\,\mathrm{d}s + \mathcal{O}(\epsilon),$$

we require the nonpositivity of $\Re(\lambda_2(m))$. Note that

$$\begin{aligned} &\int_0^{R_c-\epsilon} \left(f_s^\epsilon(s) + (f_s^\epsilon)'(s)s\right)(1-\cos(-2\pi m s))\,\mathrm{d}s \\ &= (R_c-\epsilon)\exp(-e_s(R_c-\epsilon)) - \frac{8e_s\pi^2m^2}{(4\pi^2m^2+e_s^2)^2} \\ &\quad - \frac{\exp(-e_s(R_c-\epsilon))}{(4\pi^2m^2+e_s^2)^2}\left[e_s(4\pi^2m^2(e_s(R_c-\epsilon)-2) + e_s^3(R_c-\epsilon))\cos(2\pi m(R_c-\epsilon))\right. \\ &\qquad - 2\pi m(4\pi^2m^2(e_s(R_c-\epsilon)-1) + e_s^2(e_s(R_c-\epsilon)+1))\sin(2\pi m(R_c-\epsilon)) \\ &\qquad \left. - (R_c-\epsilon)(4\pi^2m^2+e_s^2)^2\right], \end{aligned}$$

implying that we have $\int_0^{R_c-\epsilon}(f_s^\epsilon(s) + (f_s^\epsilon)'(s)s)(1-\cos(-2\pi m s))\,\mathrm{d}s > 0$ for any $\epsilon > 0$ and $m \in \mathbb{N}$ sufficiently large, i.e., high wave stability cannot be achieved. However, note that $\exp(-e_sR_c)$ can be assumed to be very small for $e_s > 0$ sufficiently large. This motivates us to consider a force coefficient function of the form

$$f_s^\epsilon \colon \mathbb{R}_+ \to \mathbb{R},$$
$$f_s^\epsilon(|d|) = \begin{cases} c\exp(-e_s|d|) - c\exp(-e_s(R_c-\epsilon)), & |d| \in [0, R_c-\epsilon], \\ -ce_s\exp(-e_s(R_c-\epsilon))\left(\frac{(|d|-R_c)^3}{\epsilon^2} + \frac{(|d|-R_c)^2}{\epsilon}\right), & |d| \in (R_c-\epsilon, R_c), \\ 0, & |d| \ge R_c, \end{cases} \tag{4.26}$$

with $c > 0$ and $e_s > 0$. Here, the first term in (4.26) represents the exponential decay of the force coefficient. To approximate the high wave number stability condition, we require $f_s(R_c - \epsilon) = 0$ which can be guaranteed by subtracting the constant $\exp(-e_s(R_c - \epsilon))$. Note that we can choose $e_s \gg 1$ such that $\exp(-e_s(R_c - \epsilon))$ is a small positive number. Subtracting the constant $c\exp(-e_s(R_c - \epsilon))$ as in (4.26) leads to $f_s^\epsilon(R_c - \epsilon) = 0$. This additional constant only changes the force coefficient f_s^ϵ slightly and does not change its derivative $(f_s^\epsilon)'$ on $[0, R_c - \epsilon]$, i.e., $f_s' = (f_s^\epsilon)'$ on $[0, R_c - \epsilon]$. Note that the differences between f_s^ϵ and f_s, and $(f_s^\epsilon)'$ and f_s' on $[R_c - \epsilon, R_c]$ are negligible provided $e_s > 0$ is chosen sufficiently large such that $e_s \exp(-e_s(R_c - \epsilon)) \ll 1$. Thus, we make the following assumption in the following.

Assumption 4.11. We assume that the purely repulsive, exponentially decaying force coefficient f_s along s is given by (4.26), i.e.,

$$f_s^\epsilon \colon \mathbb{R}_+ \to \mathbb{R},$$
$$f_s^\epsilon(|d|) = \begin{cases} c\exp(-e_s|d|) - c\exp(-e_s(R_c - \epsilon)), & |d| \in [0, R_c - \epsilon], \\ -ce_s\exp(-e_s(R_c - \epsilon))\left(\frac{(|d|-R_c)^3}{\epsilon^2} + \frac{(|d|-R_c)^2}{\epsilon}\right), & |d| \in (R_c - \epsilon, R_c), \\ 0, & |d| \geq R_c, \end{cases}$$

where $c > 0$ and $e_s \gg 1$. For the forces along l we either consider linear or exponentially decaying force coefficients. For a linear force coefficient we consider (4.18), i.e.,

$$f_l^\epsilon(|d|) := \begin{cases} a_l|d| + b_l, & |d| \in [0, R_c - \epsilon], \\ (2b_l + 2R_ca_l - a_l\epsilon)\frac{(|d|-R_c)^3}{\epsilon^3} + (3b_l + 3R_ca_l - 2a_l\epsilon)\frac{(|d|-R_c)^2}{\epsilon^2}, & |d| \in (R_c - \epsilon, R_c), \\ 0, & |d| \geq R_c, \end{cases}$$

where we assume that the parameters a_l, b_l satisfy the sign conditions $a_l < 0,\ b_l > 0$ in Assumption 4.1 as well as the necessary stability condition along l in (4.18). For an exponentially decaying force coefficient f_l^ϵ we assume that f_l^ϵ is of the form (4.23), i.e.,

$$f_l^\epsilon(|d|) = \begin{cases} c_{l_1}\exp(-e_{l_1}|d|) + c_{l_2}\exp(-e_{l_2}|d|), & |d| \in [0, R_c - \epsilon], \\ \sum_{j=1}^2(-\epsilon c_{l_j}e_{l_j} + 2c_{l_j})\exp(-e_{l_j}(R_c - \epsilon))\frac{(|d|-R_c)^3}{\epsilon^3} & \\ \quad + \sum_{j=1}^2(-\epsilon c_{l_j}e_{l_j} + 3c_{l_j})\exp(-e_{l_j}(R_c - \epsilon))\frac{(|d|-R_c)^2}{\epsilon^2}, & |d| \in (R_c - \epsilon, R_c), \\ 0, & |d| \geq R_c, \end{cases}$$

for parameters

$$c_{l_1} > 0 > c_{l_2}, \quad c_{l_1} > |c_{l_2}|, \quad \text{and} \quad e_{l_1} > e_{l_2} > 0$$

as in (4.23)–(4.24) such that the necessary stability condition (4.25) for a straight vertical line is satisfied for all $m \in \mathbb{N}$ and $0 < \epsilon \ll R_c$.

Theorem 4.12. *For the cutoff radius $R_c = 0.5$, the straight vertical line is stable for the particle model (2.9) for any $N \in \mathbb{N}$ sufficiently large with the exponentially decaying force coefficient f_s^ϵ in (4.26) along s and a linear or exponentially decaying force coefficient f_l^ϵ as*

in Assumption 4.11 along l in the limit $\epsilon \to 0$. For $R_c \in (0, 0.5)$ the straight vertical line is an unstable steady state to (2.9) for any $N \in \mathbb{N}$ sufficiently large and for the continuum limit $N \to \infty$ for any exponential decay $e_s > 0$ in the limit $\epsilon \to 0$. For any $0 < \epsilon \ll R_c$, the straight vertical lime is an unstable steady state for any $R_c \in (0, 0.5]$.

Proof. Due to the assumptions on f_l^ϵ in Assumption 4.11 the real part for the first eigenvalue in (3.13), given by

$$\Re(\lambda_1(m)) = 2\int_0^{R_c-\epsilon} f_l^\epsilon(s)\,(1-\cos(-2\pi m s))\,\mathrm{d}s + \mathcal{O}(\epsilon),$$

is not positive for any $m \in \mathbb{N}$ and any $0 < \epsilon \ll R_c$ sufficiently small. The real part of the second eigenvalue (3.13) is given by

$$\Re(\lambda_2(m)) = 2\int_0^{R_c-\epsilon} \left(f_s^\epsilon(s) + (f_s^\epsilon)'(s)s\right)(1-\cos(-2\pi m s))\,\mathrm{d}s + \mathcal{O}(\epsilon).$$

For the nonpositivity of $\Re(\lambda_2(m))$ it is sufficient to require

$$\int_0^{R_c-\epsilon} \left(f_s^\epsilon(s) + s(f_s^\epsilon)'(s)\right)(1-\cos(2\pi m s))\,\mathrm{d}s \le 0, \tag{4.27}$$

for any $\epsilon > 0$ sufficiently small where the left-hand side is given by

$$\begin{aligned}
&c\int_0^{R_c-\epsilon} (\exp(-e_s s)(1-e_s s) - \exp(-e_s(R_c-\epsilon)))\,(1-\cos(2\pi m s))\,\mathrm{d}s \\
&= -\frac{c e_s \exp(-e_s(R_c-\epsilon))}{2\pi m\,(e_s^2+4\pi^2m^2)^2}\left[2\pi m\left(e_s^3(R_c-\epsilon) + 4\pi^2m^2(e_s(R_c-\epsilon)-2)\right)\cos(2\pi m(R_c-\epsilon))\right. \\
&\quad - \left(e_s^3 + 4\pi^2 e_s^2 m^2(R_c-\epsilon) + 12\pi^2 e_s m^2 + 16\pi^4 m^4(R_c-\epsilon)\right)\sin(2\pi m(R_c-\epsilon)) \\
&\quad \left. + 16\pi^3 m^3 \exp(e_s(R_c-\epsilon))\right].
\end{aligned} \tag{4.28}$$

For $R_c = 0.5$ we have $\lim_{\epsilon\to 0}\sin(2\pi m(R_c-\epsilon)) = 0$ and the right-hand side of (4.28) simplifies to $g_\epsilon(m)h_\epsilon(m)$, where

$$\begin{aligned}
g_\epsilon(m) &= -\frac{c e_s \exp(-e_s(R_c-\epsilon))}{(e_s^2+4\pi^2m^2)^2}, \\
h_\epsilon(m) &= \left(e_s^3(R_c-\epsilon) + 4\pi^2m^2(e_s(R_c-\epsilon)-2)\right)\cos(2\pi m(R_c-\epsilon)) + 8\pi^2m^2\exp(e_s(R_c-\epsilon)).
\end{aligned}$$

For determining the limit $m \to \infty$ of $g_\epsilon(m)h_\epsilon(m)$ note that the leading order term of g_ϵ is m^{-4} while the highest order term of h_ϵ is m^2, implying that the product $g_\epsilon(m)h_\epsilon(m)$, i.e., the right-hand side of (4.28), goes to zero as $m \to \infty$.
Note that for $R_c = 0.5$ we have

$$\lim_{\epsilon\to 0}\cos(2\pi m(R_c-\epsilon)) = \begin{cases} 1, & m \text{ even}, \\ -1, & m \text{ odd}. \end{cases}$$

Let us consider $e_s > 0$ with $e_s \le 4$ first, i.e., $\lim_{\epsilon\to 0} e_s(R_c - \epsilon) \le 2$. Then,

$$\lim_{\epsilon\to 0} h_\epsilon(m) = \begin{cases} e_s^3 R_c + 4\pi^2 m^2 \left(e_s R_c - 2 + 2\exp\left(e_s R_c\right)\right), & m \text{ even}, \\ -e_s^3 R_c + 4\pi^2 m^2 \left(-e_s R_c + 2 + 2\exp\left(e_s R_c\right)\right), & m \text{ odd}. \end{cases}$$

Note that $\lim_{\epsilon\to 0} g_\epsilon(m) < 0$ for all $m \in \mathbb{N}$ and $\lim_{\epsilon\to 0} h_\epsilon(m) > 0$ for all even m since $2\exp(e_s R_c) > 2$. For m odd, note that the term in brackets is positive and a lower bound of $\lim_{\epsilon\to 0} h_\epsilon$ is given by

$$-16 e_s R_c + 4\pi^2 \left(-e_s R_c + 2 + 2\exp\left(e_s R_c\right)\right) \ge 8\pi^2 \left(-e_s R_c + 1 + \exp\left(e_s R_c\right)\right),$$

which is clearly positive. Hence, $\lim_{\epsilon\to 0} h_\epsilon(m)$ is positive for all $m \in \mathbb{N}$ and, thus, we obtain $\lim_{\epsilon\to 0} g_\epsilon(m) h_\epsilon(m) < 0$, provided $e_s \le 4$ and $R_c = 0.5$. This implies that (4.27) is satisfied for all $m \in \mathbb{N}$ in this case.

Let us now consider $\lim_{\epsilon\to 0} e_s(R_c - \epsilon) > 2$ with $R_c = 0.5$. Note that a lower bound of $\lim_{\epsilon\to 0} h_\epsilon$ is obtained from $\lim_{\epsilon\to 0} \cos(2\pi m(R_c - \epsilon)) \ge -1$, leading to the upper bound

$$\lim_{\epsilon\to 0} g_\epsilon(m) \left[-\left(e_s^3 R_c + 4\pi^2 m^2 (e_s R_c - 2)\right) + 8\pi^2 m^2 \exp\left(e_s R_c\right)\right]$$

of $\lim_{\epsilon\to 0} g_\epsilon(m) h_\epsilon(m)$ since $g_\epsilon(m) < 0$ for all $\epsilon > 0$. This upper bound can be rewritten as

$$\lim_{\epsilon\to 0} g_\epsilon(m) \left[-e_s^3 R_c + 4\pi^2 m^2 \left(-e_s R_c + 2 + 2\exp\left(e_s R_c\right)\right)\right].$$

Note that $-e_s R_c + 2 + 2\exp\left(e_s R_c\right) > 0$. Besides,

$$\frac{e_s^3 R_c}{4\pi^2 \left(-e_s R_c + 2 + 2\exp\left(e_s R_c\right)\right)} < 1$$

is satisfied for all $e_s > 4$, implying

$$-e_s^3 R_c + 4\pi^2 m^2 \left(-e_s R_c + 2 + 2\exp\left(e_s R_c\right)\right) > 0$$

for all $m \in \mathbb{N}$. Hence, the right-hand side of (4.28), i.e., $g_\epsilon(m) h_\epsilon(m)$, is negative for all $m \in \mathbb{N}$ in the limit $\epsilon \to 0$. In particular, this shows that condition (4.27) is satisfied for all $m \in \mathbb{N}$ for $R_c = 0.5$.

For $R_c \in (0, 0.5]$ and $\epsilon > 0$ we have $\sin(2\pi m(R_c - \epsilon)) > 0$ for countably many $m \in \mathbb{N}$. In particular, there exists $\delta > 0$ and a countably infinite set $\mathcal{N} \subset \mathbb{N}$ such that $\sin(2\pi m(R_c - \epsilon)) > \delta$ for all $m \in \mathcal{N}$. Hence the second term in (4.28) is negative with upper bound

$$-\left(e_s^3 + 4\pi^2 e_s^2 m^2 (R_c - \epsilon) + 12\pi^2 e_s m^2 + 16\pi^4 m^4 (R_c - \epsilon)\right)\delta < 0$$

for all $m \in \mathcal{N}$. This implies that the right-hand side of (4.28), i.e., $g_\epsilon(m), h_\epsilon(m)$, can be estimated from below by

$$\frac{g_\epsilon(m)}{2\pi m}\left[2\pi m \max\{e_s^3(R_c - \epsilon) + 4\pi^2 m^2 (e_s(R_c - \epsilon) - 2), -e_s^3(R_c - \epsilon) - 4\pi^2 m^2 (e_s(R_c - \epsilon) - 2)\}\right.$$
$$\left. + 16\pi^3 m^3 \exp\left(e_s(R_c - \epsilon)\right) - \left(e_s^3 + 4\pi^2 e_s^2 m^2 (R_c - \epsilon) + 12\pi^2 e_s m^2 + 16\pi^4 m^4 (R_c - \epsilon)\right)\delta\right]$$

for all $m \in \mathcal{N}$ and $0 < \epsilon \ll R_c$ since $g_\epsilon(m) < 0$ for all $m \in \mathbb{N}$. Thus, there exists $m_0 \in \mathcal{N}$ such that the term in square brackets is negative for all $m \in \mathcal{N}$ with $m \geq m_0$ and all $\epsilon > 0$ sufficiently small since the highest order term of power m^4 in the square brackets dominates for m large enough. In particular, $g_\epsilon(m_0) < 0$ for $\epsilon > 0$ implies that we have found a positive lower bound of the right-hand side in (4.28) and one can easily show that this positive lower bound also holds in the limit $\epsilon \to 0$. Hence, stability cannot be achieved in the case $R_c \in (0, 0.5]$, and any $\epsilon > 0$, as well as for $R_c \in (0, 0.5)$ and $\epsilon \to 0$, both for $N \in \mathbb{N}$ sufficiently large and in the continuum limit $N \to \infty$. ∎

Remark 4.13. For $R_c \in (0, 0.5)$ and $\epsilon \to 0$, no stability can be shown analytically. However, note that an upper bound of the integral

$$\int_0^{R_c-\epsilon} \left(f_s^\epsilon(s) + s(f_s^\epsilon)'(s)\right)(1 - \cos(2\pi m s))\,\mathrm{d}s \tag{4.29}$$

in the necessary stability condition (4.27) is given by

$$\begin{aligned}
&-\frac{c e_s \exp\left(-e_s(R_c-\epsilon)\right)}{2\pi m \left(e_s^2 + 4\pi^2 m^2\right)^2}\left[-2\pi m\left(e_s^3(R_c-\epsilon) + 4\pi^2 m^2(e_s(R_c-\epsilon) - 2)\right)\right.\\
&\left.-\left(e_s^3 + 4\pi^2 e_s^2 m^2(R_c-\epsilon) + 12\pi^2 e_s m^2 + 16\pi^4 m^4(R_c-\epsilon)\right) + 16\pi^3 m^3 \exp\left(e_s(R_c-\epsilon)\right)\right]\\
&= -\frac{c e_s \exp\left(-e_s(R_c-\epsilon)\right)}{2\pi m \left(e_s^2 + 4\pi^2 m^2\right)^2}\left[-e_s^3 - 2\pi e_s^3(R_c-\epsilon)m - \left(4\pi^2 e_s^2(R_c-\epsilon) + 12\pi^2 e_s\right) m^2\right.\\
&\left.+\left(-8\pi^3(e_s(R_c-\epsilon) - 2) + 16\pi^3 \exp\left(e_s(R_c-\epsilon)\right)\right) m^3 - 16\pi^4(R_c-\epsilon)m^4\right]
\end{aligned} \tag{4.30}$$

for any $0 < \epsilon \ll R_c$ due to (4.28). For $\exp(e_s R_c) \gg 1$ there exists $m_0 \in \mathbb{N}$ of order $\exp(e_s R_c) \gg 1$ such that the term $16\pi^3 m^3 \exp(e_s R_c)$ is the dominating term in the upper bound (4.30) of the integral (4.29) for all $m \in \mathbb{N}$ with $m \leq m_0$. Hence negativity of the upper bound (4.30) and thus of the integral (4.29) in the necessary stability condition can be guaranteed for all $m \leq m_0$. For $m > m_0$, however, the highest order term of power m^4 dominates the sum. Since $m_0 \gg 1$, we have stability for $N \in \mathbb{N}$ sufficiently large and for the continuum limit $N \to \infty$ for almost all, but finitely many, Fourier modes for $e_s \gg 1$, $R_c \in (0, 0.5)$, and any $\epsilon > 0$ sufficiently small or in the limit $\epsilon \to 0$.

The integral (4.29) is explicitly evaluated in (4.28). For large values of $m \in \mathbb{N}$ the highest order term in (4.28) is associated with the summand $16\pi^4 m^4(R_c - \epsilon)\sin(2\pi m(R_c - \epsilon))$ and can be written in the form

$$\frac{8\pi^3 e_s \exp(-e_s(R_c-\epsilon))(R_c-\epsilon)m^3 \sin(2\pi m(R_c-\epsilon))}{\left(e_s^2 + 4\pi^2 m^2\right)^2}.$$

Here, the numerator increases as m^3 for large m while the denominator is of order m^4, multiplied by a factor $\exp(-e_s R_c) \ll 1$, leading to decaying sinusoidal oscillations around zero as m increases. Since this approximation is only valid for $m > m_0 \gg 1$ the absolute value of the right-hand side in (4.28) may be so small that it is numerically zero and one may see stable vertical line patterns for exponentially decaying force coefficients f_s^ϵ along s for $R_c \in (0, 0.5)$, $\epsilon > 0$ or in the limit $\epsilon \to 0$, and $N \in \mathbb{N}$ sufficiently large; see the numerical experiment in Figure 6(E).

Corollary 4.14. *Let $c_1, c_2 \in \mathbb{R}$ with $c_1 > 0$, $c_1 > |c_2|$ be given. There exist parameters $e_2 \geq e_1 > 0$ such that the straight vertical line is stable for the particle model (2.9) for $N \in \mathbb{N}$ sufficiently large for the exponentially decaying force coefficient f_s^ϵ along s given by $f_s^\epsilon \colon \mathbb{R}_+ \to \mathbb{R}$ with*

$$f_s^\epsilon(|d|) = \begin{cases} c_1 \exp(-e_1|d|) + c_2 \exp(-e_2|d|) - c, & |d| \in [0, R_c - \epsilon], \\ (f_s^\epsilon)'(R_c - \epsilon)\left(\frac{(|d|-R_c)^3}{\epsilon^2} + \frac{(|d|-R_c)^2}{\epsilon}\right), & |d| \in (R_c - \epsilon, R_c), \\ 0, & |d| \geq R_c, \end{cases} \tag{4.31}$$

with

$$c = c_1 \exp(-e_1(R_c - \epsilon)) + c_2 \exp(-e_2(R_c - \epsilon))$$

and a linear or an exponential force coefficient f_l^ϵ along l as in Assumption 4.11 for a cutoff radius $R_c = 0.5$. For the continuum limit $N \to \infty$, stability/instability cannot be concluded.

Proof. For the stability of the straight vertical line for $N \in \mathbb{N}$ sufficiently large we require that the force coefficient f_s^ϵ in (4.31) is purely repulsive for any $\epsilon > 0$ and hence at least one of the constants c_1, c_2 has to be positive. Since we can assume $c_1 > 0$ without loss of generality this implies that c_1 is a repulsive multiplicative factor, while the sign of c_2 is not given by the assumptions. Thus, we require that the first term in the definition of f_s^ϵ in (4.31) decays slower than the second one, implying $0 < e_1 \leq e_2$. Hence, the conditions on the parameters are verified.

As in the proof of Theorem 4.12 we evaluate integrals of the form (4.28) where the term with factor $\sin(2\pi m R_c)$ vanishes for our choice of $R_c = 0.5$. If $c_2 \geq 0$ one can choose e_1, e_2 sufficiently large such that the term $16\pi^3 m^3 \exp(e_k R_c), k = 1, 2$, in the square brackets in (4.28) dominates as in the proof of Theorem 4.12, leading to the stability of the vertical straight line for $N \in \mathbb{N}$ sufficiently large. For $c_2 < 0$ one can choose e_1, e_2 sufficiently large such that the term $16\pi^3 m^3 \exp(e_k R_c), k = 1, 2$, dominates the square brackets. However, since $c_1 > 0 > c_2$ we require in addition that the term with multiplicative factor c_1 dominates over the term with multiplicative factor c_2, leading to the condition

$$\begin{aligned} &- \frac{c_1 e_1 \exp(-e_1 R_c)}{2\pi m \left(e_1^2 + 4\pi^2 m^2\right)^2} \left[16\pi^3 m^3 \exp(e_1 R_c)\right] + \frac{|c_2| e_2 \exp(-e_2 R_c)}{2\pi m \left(e_2^2 + 4\pi^2 m^2\right)^2} \left[16\pi^3 m^3 \exp(e_2 R_c)\right] \\ &= - \frac{16\pi^3 m^3 c_1 e_1}{2\pi m \left(e_1^2 + 4\pi^2 m^2\right)^2} + \frac{16\pi^3 m^3 |c_2| e_2}{2\pi m \left(e_2^2 + 4\pi^2 m^2\right)^2} < 0 \end{aligned}$$

in the limit $\epsilon \to 0$ which is equivalent to

$$-c_1 e_1 \left(e_2^2 + 4\pi^2 m^2\right)^2 + |c_2| e_2 \left(e_1^2 + 4\pi^2 m^2\right)^2 < 0.$$

Since $c_1 > |c_2|$ and $e_2 \geq e_1 > 0$ by assumption this condition is satisfied for $e_2 > e_1$ sufficiently large. Hence, stability of the straight vertical line can be achieved for $N \in \mathbb{N}$ sufficiently large. ∎

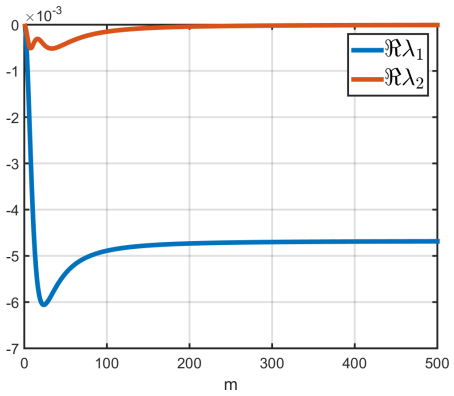

Figure 3. *$\Re(\lambda_i)$ in (3.13) as a function of m for the force coefficients f_R^ϵ in (4.32) and f_A^ϵ in (4.33) of repulsion force (2.2) and attraction force (2.3), respectively, for parameter values in (2.13) in the limit $\epsilon \to 0$, where $f_l^\epsilon = f_A^\epsilon + f_R^\epsilon$ and $f_s^\epsilon = \chi f_A^\epsilon + f_R^\epsilon$.*

The force coefficient f_s^ϵ of the form (4.31) along s is motivated by the force coefficients in the Kücken–Champod model. Here, $f_s^\epsilon = \chi f_A^\epsilon + f_R^\epsilon$ for $\chi \in [0,1]$ where, motivated by this section, $f_R^\epsilon, f_A^\epsilon$ are defined as

$$f_R^\epsilon(|d|) = \begin{cases} f_R(|d|) - f_R(R_c - \epsilon), & |d| \in [0, R_c - \epsilon], \\ f_R'(R_c - \epsilon)\left(\frac{(|d|-R_c)^3}{\epsilon^2} + \frac{(|d|-R_c)^2}{\epsilon}\right), & |d| \in (R_c - \epsilon, R_c), \\ 0, & |d| \geq R_c, \end{cases} \tag{4.32}$$

and

$$f_A^\epsilon(|d|) = \begin{cases} f_A(|d|) - f_A(R_c - \epsilon), & |d| \in [0, R_c - \epsilon], \\ f_A'(R_c - \epsilon)\left(\frac{(|d|-R_c)^3}{\epsilon^2} + \frac{(|d|-R_c)^2}{\epsilon}\right), & |d| \in (R_c - \epsilon, R_c), \\ 0, & |d| \geq R_c. \end{cases} \tag{4.33}$$

This corresponds to the sum of an attractive and a repulsive force coefficient as in (4.31) for $c_1 > 0 > c_2$ where the repulsive term, i.e., $c_1 > |c_2|$, dominates. This motivates that we obtain stability of the straight vertical line for the force coefficients in the Kücken–Champod model for $N \in \mathbb{N}$ sufficiently large by considering force coefficients of the form (4.32), (4.33).

4.4. Kücken–Champod model. For the specific forces in the Kücken–Champod model, given by the repulsive and attractive force coefficients f_R^ϵ and f_A^ϵ in (4.32) and (4.33), respectively, we require the nonpositivity of the real parts of the eigenvalues $\lambda_k, k = 1, 2$, given by

$$\begin{aligned} \Re(\lambda_1(m)) &= 2\int_0^{R_c} f_l^\epsilon(s)\,(1 - \cos(-2\pi m s))\,\mathrm{d}s, \\ \Re(\lambda_2(m)) &= 2\int_0^{R_c} \left(f_s^\epsilon(s) + s(f_s^\epsilon)'(s)\right)(1 - \cos(-2\pi m s))\,\mathrm{d}s \end{aligned}$$

in (3.13) where $f_l^\epsilon = f_A^\epsilon + f_R^\epsilon$ and $f_s^\epsilon = \chi f_A^\epsilon + f_R^\epsilon$. In Figure 3 we evaluate $\Re(\lambda_k)$ numerically for the force coefficients (4.32) and (4.33) in the Kücken–Champod model for the parameters

in (2.13) and a cutoff radius $R_c = 0.5$ in the limit $\epsilon \to 0$. Clearly, $\Re(\lambda_1) \leq 0$, while $\Re(\lambda_2)$ is negative for small modes m but tends to zero for large modes m.

Investigating the high wave number stability for the forces in the Kücken–Champod model can be done analytically. For the general necessary high wave number condition (3.17) for λ_1 we require

$$\int_0^{R_c} f_l^\epsilon \, \mathrm{d}s \leq 0.$$

Note that

$$\begin{aligned}
&\lim_{\epsilon\to 0} \int_0^{R_c-\epsilon} \exp(-e_R s)\left(\alpha s^2 + \beta\right) - \gamma \exp(-e_A s) s \, \mathrm{d}s \\
&= \frac{\alpha\left(\exp(-e_R R_c)(-e_R R_c(e_R R_c + 2) - 2) + 2\right)}{(e_R)^3} + \frac{\beta - \beta\exp(-e_R R_c)}{e_R} \\
&\quad - \frac{\gamma\left(1 - \exp(-e_A R_c)(e_A R_c + 1)\right)}{(e_A)^2} \\
&\approx \frac{2\alpha}{(e_R)^3} + \frac{\beta}{e_R} - \frac{\gamma}{(e_A)^2}
\end{aligned}$$

which is clearly negative for the choice of parameters in (2.13). For the high wave stability we also consider the condition associated with λ_2, leading to the condition

$$\int_0^{R_c} f_s^\epsilon(s) + s(f_s^\epsilon)'(s) \, \mathrm{d}s \leq 0.$$

We evaluate the integral

$$\begin{aligned}
&\int_0^{R_c-\epsilon} \exp(-e_R s)\left(\alpha\left(3s^2 - e_R s^3\right) + \beta(1 - e_R s)\right) - \chi\gamma \exp(-e_A s) s(2 - e_A s) \, \mathrm{d}s \\
&= (R_c - \epsilon)\left[(R_c - \epsilon)\left[\alpha(R_c - \epsilon)\exp(-e_R(R_c - \epsilon)) - \chi\gamma\exp(-e_A(R_c - \epsilon))\right]\right. \\
&\qquad \left. + \beta\exp(-e_R(R_c - \epsilon))\right] \\
&= (R_c - \epsilon)\left(f_R(R_c - \epsilon) + \chi f_A(R_c - \epsilon)\right)
\end{aligned}$$

for f_R and f_A defined in (2.11) and (2.12), respectively, implying that

$$\int_0^{R_c-\epsilon} f_s^\epsilon(s) + s(f_s^\epsilon)'(s) \, \mathrm{d}s = 0$$

for any $\epsilon > 0$. In particular, the straight vertical line is high wave number stable for any $N \in \mathbb{N}$ sufficiently large and in the continuum limit $N \to \infty$ for the Kücken–Champod model with force coefficients f_R^ϵ and f_A^ϵ in (4.32) and (4.33), respectively, the parameters in (2.13), and $\epsilon \to 0$. By definition of $f_s^\epsilon = \chi f_A^\epsilon + f_R^\epsilon$, we have $f_s^\epsilon(R_c) = 0$, i.e., the high wave number stability of the straight vertical line (compare Proposition 3.5), is satisfied. Note that

$$\lim_{\epsilon\to 0} \chi f_A(R_c - \epsilon) + f_R(R_c - \epsilon) = 4.8144 \cdot 10^{-21}$$

Table 1

Stability/instability of the straight vertical line (3.3) for the particle model (2.9) with force coefficients f_s along s and different cutoff radii $R_c \in (0, 0.5]$.

Force coefficient f_s along s	$R_c \in (0, 0.5)$	$R_c = 0.5$
Linear force coefficient (4.1)	Instability for any $N \in \mathbb{N}$ sufficiently large and for $N \to \infty$ (see Theorem 4.5)	Stability or instability since stability conditions are satisfied with equality (see Remark 4.6)
Algebraically decaying force coefficient (4.20)	Instability for any $N \in \mathbb{N}$ sufficiently large and for $N \to \infty$ (see Corollary 4.10)	Instability for any $N \in \mathbb{N}$ sufficiently large and for $N \to \infty$ (see Corollary 4.10)
Exponentially decaying force coefficient (4.26)	Instability for any $N \in \mathbb{N}$ sufficiently large and for $N \in \mathbb{N}$ (see Theorem 4.12), but stability may be seen in numerical simulations (see Remark 4.13)	Stability for any $N \in \mathbb{N}$ sufficiently large (see Theorem 4.12)

for $R_c = 0.5$, i.e., the force coefficient $\chi f_A + f_R$ has only slightly been modified to obtain $\chi f_A^\epsilon + f_R^\epsilon$ with $(\chi f_A^\epsilon + f_R^\epsilon)' \approx (\chi f_A^\epsilon + f_R^\epsilon)'$, provided $e_R \exp(-e_R R_c) \ll 1$ and $e_A \exp(-e_A R_c) \ll 1$.

Note that it is not possible to analyze the stability of the straight vertical line for all modes $m \in \mathbb{N}$ for the forces f_R^ϵ and f_A^ϵ in (4.32) and (4.33) in the Kücken–Champod model analytically for all possible parameter values due to the large number of parameters in the model. Besides, the force coefficients strongly depend on the choice of parameters. In Corollary 4.14, however, we investigated the stability of the straight vertical line for $N \in \mathbb{N}$ sufficiently large where f_s^ϵ, restricted to $[0, R_c - \epsilon]$ for some $\epsilon > 0$, is the sum of the positive term $c_1 \exp(-e_1|d|)$, the negative term $c_2 \exp(-e_2|d|)$, and a constant to guarantee $f_s^\epsilon(R_c - \epsilon) = 0$, where $c_1 > |c_2| > 0$. Besides, we required $e_1 < e_2$ for the positivity of the sum $c_1 \exp(-e_1|d|) + c_2 \exp(-e_2|d|)$ for $|d| \in [0, R_c - \epsilon]$ and showed stability of the straight vertical line for $N \in \mathbb{N}$ sufficiently large provided the parameters $e_1, e_2 > 0$ are chosen sufficiently large enough. In Figure 1 the absolute value of the terms χf_A and f_R, defined in (2.11)–(2.12), are plotted for the parameters in (2.13). As in Corollary 4.14 the positive term always dominates and the terms χf_A and f_R have fast exponential decays. This suggests that the straight vertical line is a stable steady state for the Kücken–Champod model for $N \in \mathbb{N}$ sufficiently large with the adopted force coefficient $f_s^\epsilon = \chi f_A^\epsilon + f_R^\epsilon$. Besides, the numerical evaluation of the real part of the eigenvalue λ_2 for f_s^ϵ for $\epsilon > 0$, i.e., a differentiable force coefficient with the additional constant $-(\chi f_A(R_c - \epsilon) + f_R(R_c - \epsilon))$ for $|d| \in [0, R_c - \epsilon]$ leads to nonpositivity of the real part of the eigenvalue λ_2.

4.5. Summary. In this section, we summarize the results from the previous subsections on the stability of the straight vertical line (3.3) of the particle model (2.9) with linear, algebraically decaying, and exponentially decaying force coefficients for different values of the cutoff radius $R_c \in (0, 0.5]$. This summary is shown in Table 1.

5. Numerical simulations.

5.1. Numerical methods. As in [17, 36] we consider the unit square with periodic boundary conditions as the domain for our numerical simulations if not stated otherwise. The particle system (2.9) is solved by either the simple explicit Euler scheme or higher order methods such as the Runge–Kutta–Dormand–Prince method, all resulting in very similar simulation results. Note that the time step has to be adjusted depending on the value of the cutoff radius R_c. For efficient numerical simulation we consider cell lists as outlined in [36].

5.2. Numerical results. Numerical results are shown in Figures 4–9. For all numerical simulations we consider $N = 600$ particles which are initially equiangular distributed on a circle with center $(0.5, 0.5)$ and radius 0.005 as illustrated in Figure 4(A). The stationary solution for the linear force coefficient f_s^ϵ in (4.1), i.e.,

$$f_s^\epsilon(|d|) = a_s|d| + b_s, \qquad f_l^\epsilon(|d|) = 0.1 - 3|d|, \qquad |d| \in [0, R_c - \epsilon],$$

for different values of a_s, b_s, is shown in Figure 4 in the limit $\epsilon \to 0$. As proven in section 4.1 equidistantly distributed particles along the vertical straight line form an unstable steady state for $N \in \mathbb{N}$ sufficiently large for $R_c \in (0, 0.5)$. Hence, the stationary solutions are no lines of uniformly distributed particles and we obtain different clusters or line patterns instead. In Figure 4(B), we consider $R_c = 0.3$, resulting in clusters of particles along the vertical axis. For $R_c = 0.5$ and a_s, b_s chosen as $a_s = -\frac{b_s}{R_c}$, the requirement in (4.18) for the necessary stability condition to be satisfied with equality, the real part of one of the eigenvalues of the stability matrix is equal to zero. The resulting steady states are shown for different scalings of the parameters a_s, b_s in Figures 4(C) and 4(D). One can see that the particles align along a vertical line along the entire interval $[0, 1]$, but are not equidistantly distributed along the vertical axis and thus the vertical straight line is an unstable steady state for any $N \in \mathbb{N}$ sufficiently large. For $a_s > -\frac{b_s}{R_c}$ and $a_s < -\frac{b_s}{R_c}$, respectively, with $R_c = 0.5$ the corresponding steady states are shown in Figures 4(E) and 4(F), resulting in clusters along the vertical axis.

In Figure 5, we consider the linear force coefficient f_s^ϵ in (4.1) for different values of a_s, b_s, and R_c, where $\epsilon = 0.01$ is fixed in contrast to $\epsilon \to 0$ in Figure 4, i.e., we consider the total force (2.7) with linear force coefficients $f_l^\epsilon(|d|) = a_l|d| + b_l$, $f_s^\epsilon(|d|) = a_s|d| + b_s$ for $|d| \in [0, R_c - \epsilon]$ in (4.1) with $a_l = -3, b_l = 0.1$. In Figure 5(A), we consider the same parameter values as in Figure 4(B), i.e., $a_s = -0.2, b_s = 0.1$, and $R_c = 0.3$, resulting in the same stationary solution for $\epsilon = 0.01$ and $\epsilon \to 0$. In particular, the straight vertical line is unstable both for $\epsilon = 0.01$ and $\epsilon \to 0$. For cutoff radius $R_c = 0.5$, we obtain different stationary solutions for $\epsilon = 0.01$ and $\epsilon \to 0$. In Figure 5(B), we show the stationary solutions for $a_s = -0.2, b_s = 0.1$, and $R_c = 0.5$ as in Figure 4(C), i.e., $a_s = -\frac{b_s}{R_c}$. Even though stability/instability could not be determined analytically the numerical results illustrate that straight vertical line is unstable both for $\epsilon = 0.01$ and $\epsilon \to 0$. The stationary solution for $a_s = -0.1, b_s = 0.1$, and $R_c = 0.5$ is shown in Figure 5(C) for $\epsilon = 0.01$ and in Figure 4(E) for $\epsilon \to 0$. Our analytical results show that the stationary solution is unstable in this case which is also consistent with the numerical results. In particular, we obtain the same instability results for $\epsilon = 0.01$ as in Figure 4 where the limit $\epsilon \to 0$ is considered.

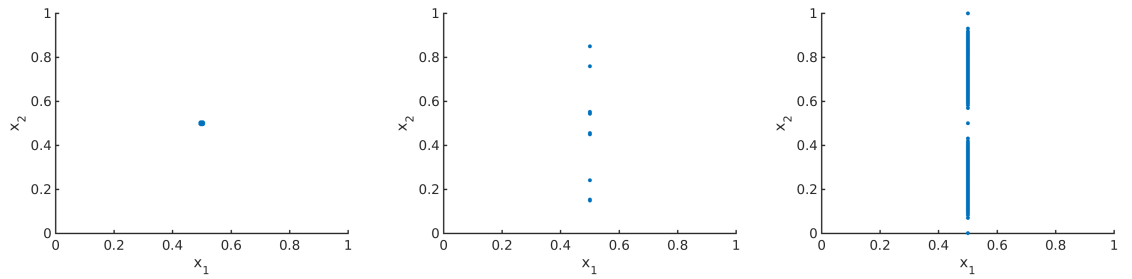

(A) Initial data (B) $a_s = -0.2$, $b_s = 0.1$, $R_c = 0.3$ (C) $a_s = -0.2$, $b_s = 0.1$, $R_c = 0.5$

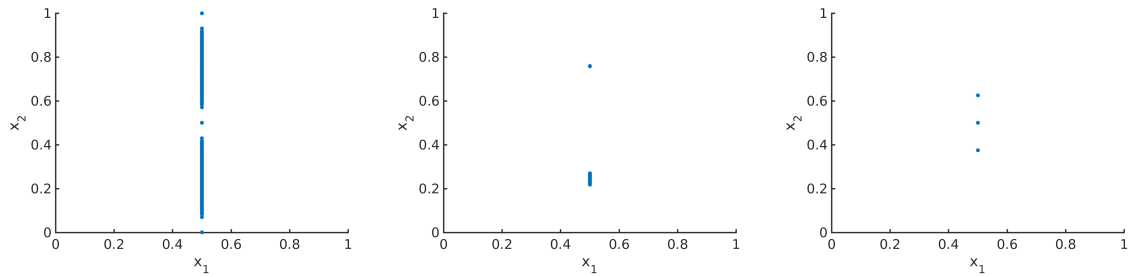

(D) $a_s = -0.02$, $b_s = 0.01$, $R_c = 0.5$ (E) $a_s = -0.1$, $b_s = 0.1$, $R_c = 0.5$ (F) $a_s = -0.4$, $b_s = 0.1$, $R_c = 0.5$

Figure 4. *Stationary solution to the model (2.9) for total force (2.7) with linear force coefficients $f_l^\epsilon(|d|) = a_l|d| + b_l$, $f_s^\epsilon(|d|) = a_s|d| + b_s$ for $|d| \in [0, R_c - \epsilon]$ in (4.1) with $a_l = -3, b_l = 0.1$, and cutoff radius R_c in the limit $\epsilon \to 0$.*

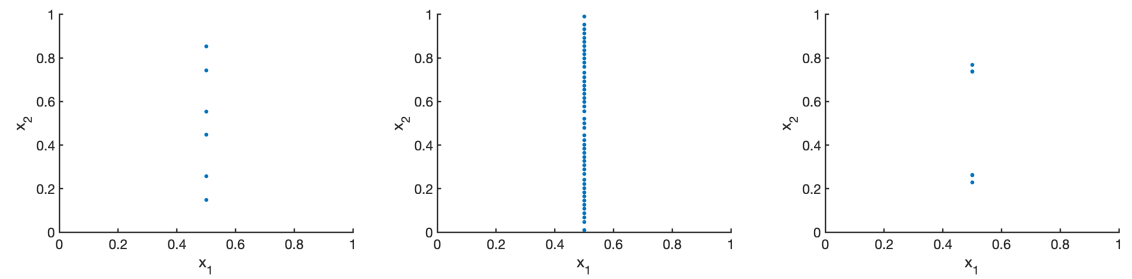

(A) $a_s = -0.2$, $b_s = 0.1$, $R_c = 0.3$ (B) $a_s = -0.2$, $b_s = 0.1$, $R_c = 0.5$ (C) $a_s = -0.1$, $b_s = 0.1$, $R_c = 0.5$

Figure 5. *Stationary solution to the model (2.9) for total force (2.7) with linear force coefficients $f_l^\epsilon(|d|) = a_l|d| + b_l$, $f_s^\epsilon(|d|) = a_s|d| + b_s$ for $|d| \in [0, R_c - \epsilon]$ in (4.1) with $a_l = -3, b_l = 0.1$, and cutoff radius R_c for $\epsilon = 0.01$.*

For the exponentially decaying force coefficient f_s^ϵ along s in (4.26), given by

$$f_s^\epsilon(|d|) = c\exp(-e_s|d|) - c\exp(-e_s(R_c - \epsilon)), \qquad |d| \in [0, R_c - \epsilon],$$

for $\epsilon > 0$, we consider the parameter values $c = 0.1$ and $e_s = 100$ if not stated otherwise. The initial data are given by equiangular distributed particles on a circle with center $(0.5, 0.5)$ and radius 0.005 in Figure 6(A). In Figures 6(B)–6(F) the stationary solution for the exponentially

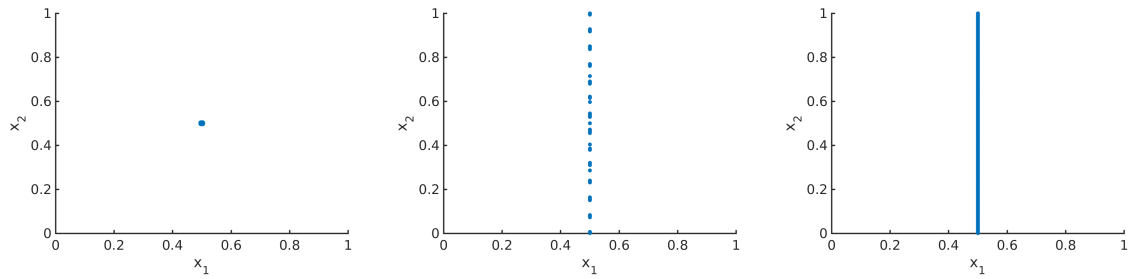

(A) Initial data (B) $e_s = 10$, $R_c = 0.1$, f_l linear (C) $e_s = 10$, $R_c = 0.5$, f_l linear

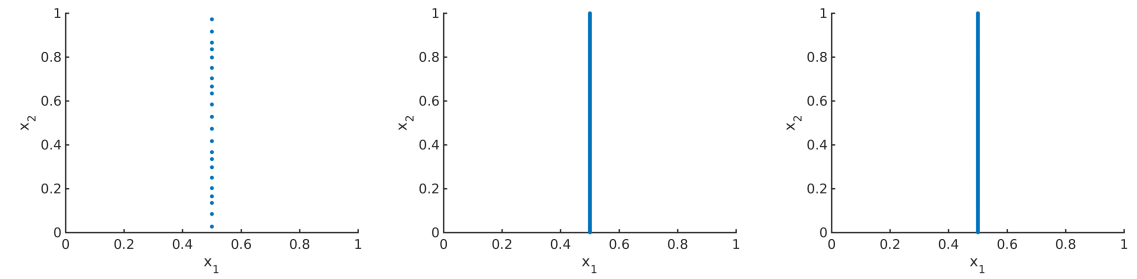

(D) $e_s = 10$, $R_c = 0.5$, f_l linear, no add. constant for f_s (E) $e_s = 100$, $R_c = 0.1$, f_l linear (F) $e_s = 100$, $R_c = 0.5$, f_l exp.

Figure 6. *Stationary solution to the model (2.9) for total force (2.7) with exponential force coefficient* $f_s^\epsilon(|d|) = c\exp(-e_s|d|) - c\exp(-e_s(R_c-\epsilon))$ *for* $|d| \in [0, R_c-\epsilon]$ *along* s*, defined in (4.26), and* $f_l^\epsilon(|d|) = 0.1-3|d|$ *or* $f_l^\epsilon(|d|) = 0.13\exp(-100|d|) - 0.03\exp(-10|d|)$ *for* $|d| \in [0, R_c-\epsilon]$ *along* l *with cutoff* R_c *in the limit* $\epsilon \to 0$.

decaying force coefficient f_s^ϵ in the limit $\epsilon \to 0$ is shown. As expected, for small values of e_s and $R_c \in (0, 0.5)$, e.g., $e_s = 10$, as in Figure 6(B), the equidistantly distributed particles along the vertical axis are an unstable steady state. In this case, the steady state is given by clusters along the vertical axis and $\Re(\lambda_2(m)) \le 0$ for $m < 12$ only. For $R_c = 0.5$ the straight vertical line is stable as shown in Figure 6(C). Note that the additional constant in the definition of f_s^ϵ leads to $f_s^\epsilon(R_c - \epsilon) = f_s^\epsilon(R_c) = 0$ and is necessary for the stability of the straight vertical line. In Figure 6(D) we consider f_s^ϵ without this additional constant, i.e., $f_s^\epsilon(|d|) = c\exp(-e_s|d|)$ for $|d| \in [0, R_c - \epsilon]$, where the straight vertical line is clearly unstable and we have $\Re(\lambda_2(m)) \le 0$ for $m < 9$ only. If e_s is chosen sufficiently large, e.g., $e_s = 100$ as in Figures 6(E) and 6(F), the straight vertical line appears to be stable even for $R_c < 0.5$. An explicit calculation of the eigenvalues for $R_c = 0.1$ reveals, however, that $\Re(\lambda_2(m)) \le 0$ for $m < 73723$ only. Note that we obtain stability for a much larger number of modes as in Figures 6(B) and 6(D). This is also consistent with a straight vertical line as steady state in Figure 6(F), while we have clusters as steady states in Figures 6(B) and 6(D). Further note that $\Re(\lambda_2(73723)) = 8.3225 \cdot 10^{-15}$ and hence it is numerically zero. As discussed in Remark 4.13 this explains why for $\exp(e_s R_c) \gg 1$, e.g., $e_s = 100$ and $R_c = 0.1$, the straight vertical line appears to be stable. Finally, we also obtain the straight vertical line as a steady state if we consider exponentially decaying force coefficients $f_l^\epsilon(|d|) = 0.13\exp(-100|d|) - 0.03\exp(-10|d|)$ instead of $f_l^\epsilon(|d|) = 0.1 - 3|d|$ for $|d| \in [0, R_c - \epsilon]$ in the limit $\epsilon \to 0$ as shown in Figure 6(F).

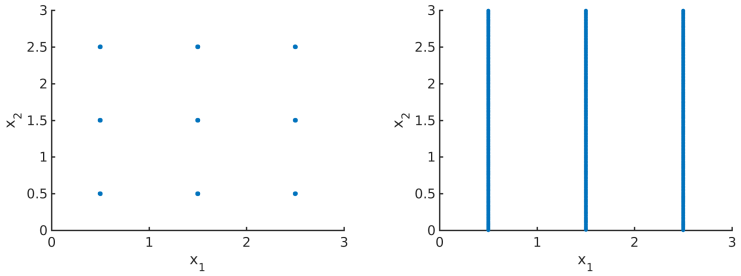

(A) Initial data (B) $R_c = 0.1$

Figure 7. *Stationary solution to the model* (2.9) *for total force* (2.7) *with exponential force coefficients* $f_s^\epsilon(|d|) = c\exp(-e_s|d|) - c\exp(-e_s(R_c-\epsilon))$ *in* (4.26) *and* $f_l^\epsilon(|d|) = 0.13\exp(-100|d|) - 0.03\exp(-10|d|)$ *with cutoff* R_c *on the domain* $[0,3]^2$.

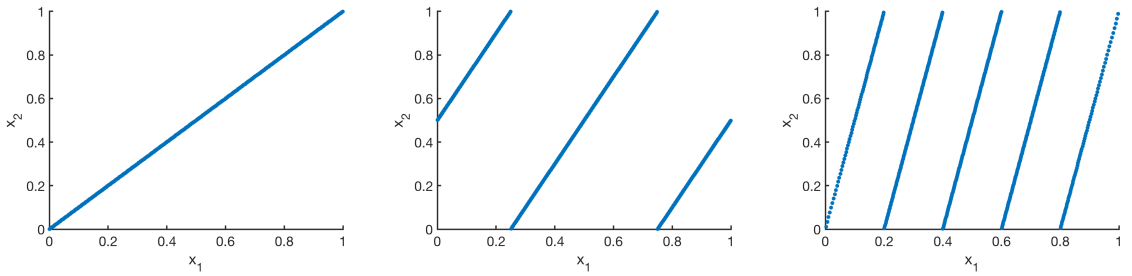

(A) $s = (1,1)/\sqrt{2}$, $l = (-1,1)/\sqrt{2}$ (B) $s = (1,2)/\sqrt{5}, l = (-2,1)/\sqrt{5}$ (C) $s = (1,5)/\sqrt{26}, l = (-5,1)/\sqrt{26}$

Figure 8. *Stationary solution to the model* (2.9) *for different tensor fields* T, *given by* s, l, *and total force* (2.7) *with exponential force coefficients* $f_s^\epsilon(|d|) = c\exp(-e_s|d|) - c\exp(-e_s(R_c-\epsilon))$ *for* $|d| \in [0, R_c-\epsilon]$ *in* (4.26) *and* $f_l^\epsilon(|d|) = 0.13\exp(-100|d|) - 0.03\exp(-10|d|)$ *for* $|d| \in [0, R_c-\epsilon]$ *with cutoff* $R_c = 0.1$ *in the limit* $\epsilon \to 0$.

Note that we also obtain a straight vertical line as a stationary solution in Figures 6(E) and 6(F) if $f_s^\epsilon(|d|) = c\exp(-e_s|d|) - c\exp(-e_s(R_c-\epsilon))$ for $|d| \in [0, R_c-\epsilon]$ is replaced by $f_s^\epsilon(|d|) = c\exp(-e_s|d|)$ since $\exp(-e_s R_c) \ll 1$ for $e_s \gg 1$.

In Figure 7 the stationary solution is shown on the domain $[0,3]^2$ instead of the unit square. Here, we consider the same force coefficients as in Figure 6(F), i.e., exponentially decaying force coefficients along l and s. We define the initial data on $[0,3]^2$ by considering the initial data on the unit square, i.e., equiangular distributed particles on a circle with center $(0.5, 0.5)$ and radius 0.005, and extending these initial conditions to $[0,3]^2$ by using the periodic boundary conditions. As expected we obtain three parallel lines as the stationary solution.

For the underlying tensor field T with $s = (0,1)$ and $l = (1,0)$, we have seen that vertical straight patterns are stable. More generally, stripe states along any angle can be obtained by rotating the spatially homogeneous tensor field T appropriately. Examples of rotated stripe patterns are shown in Figure 8 where the vector fields $s = (1,1)/\sqrt{2}, l = (-1,1)/\sqrt{2}$ in Figure 8(A), $s = (1,2)/\sqrt{5}, l = (-2,1)/\sqrt{5}$ in Figure 8(B), and $s = (1,5)/\sqrt{26}, l = (-5,1)/\sqrt{26}$ in Figure 8(C) are considered. Due to the periodicity of the forces, the resulting patterns are also periodic.

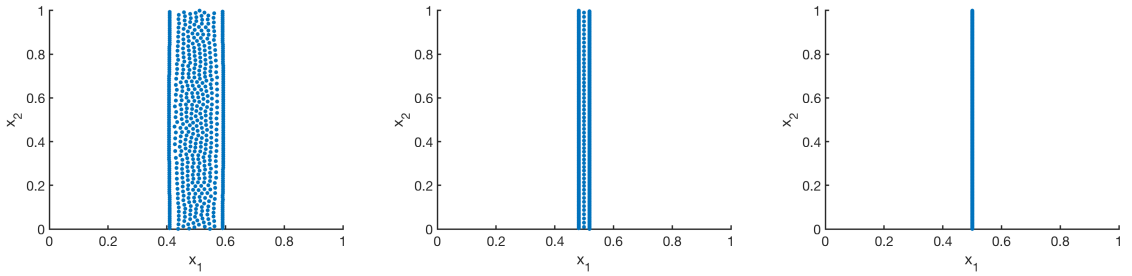

(A) $e_{l_1} = 20$ (B) $e_{l_1} = 30$ (C) $e_{l_1} = 50$

Figure 9. *Stationary solution to the model (2.9) for tensor field T with $s = (0, 1), l = (1, 0)$ and total force (2.7) with exponential force coefficients $f_s^\epsilon(|d|) = c\exp(-e_s|d|) - c\exp(-e_s(R_c - \epsilon))$ for $|d| \in [0, R_c - \epsilon]$, defined in (4.26), and $f_l^\epsilon(|d|) = 0.13\exp(-e_{l_1}|d|) - 0.03\exp(-10|d|)$ for $|d| \in [0, R_c - \epsilon]$ with cutoff $R_c = 0.5$.*

Until now, we looked at numerical examples for a stable state aligned along a line (or lines). However, the model (2.9) is also able to produce two-dimensional states which can result as an instability of a vertical line. To obtain two-dimensional patterns, we vary the force along l. In particular, the force along l has to be less attractive to avoid the concentration along line patterns. In Figure 9, we vary parameter e_{l_1} in the force coefficient $f_l^\epsilon(|d|) = 0.13\exp(-e_{l_1}|d|) - 0.03\exp(-10|d|)$ for $|d| \in [0, R_c - \epsilon]$. Here, smaller values of e_{l_1} lead to stronger repulsive forces over a short distance, resulting in a horizontal spreading of the solution for the tensor field T with $s = (0, 1)$ and $l = (1, 0)$.

REFERENCES

[1] G. Albi, D. Balagué, J. A. Carrillo, and J. von Brecht, *Stability analysis of flock and mill rings for second order models in swarming*, SIAM J. Appl. Math., 74 (2014), pp. 794–818.

[2] L. A. Ambrosio, N. Gigli, and G. Savaré, *Gradient Flows in Metric Spaces and in the Space of Probability Measures*, Lectures in Math., Birkhäuser, Basel, 2005.

[3] D. Balagué, J. A. Carrillo, T. Laurent, and G. Raoul, *Dimensionality of local minimizers of the interaction energy*, Arch. Ration. Mech. Anal., 209 (2013), pp. 1055–1088.

[4] D. Balagué, J. A. Carrillo, T. Laurent, and G. Raoul, *Nonlocal interactions by repulsive-attractive potentials: Radial ins/stability*, Phys. D, 260 (2013), pp. 5–25.

[5] D. Balagué, J. A. Carrillo, and Y. Yao, *Confinement for repulsive-attractive kernels*, Discrete Contin. Dyn. Syst. Ser. B, 19 (2014), pp. 1227–1248.

[6] P. Ball, *Nature's Patterns: A Tapestry in Three Parts*, Oxford University Press, Oxford, 2009.

[7] M. Ballerini, N. Cabibbo, R. Candelier, A. Cavagna, E. Cisbani, I. Giardina, V. Lecomte, A. Orlandi, G. Parisi, A. Procaccini, M. Viale, and V. Zdravkovic, *Interaction ruling animal collective behaviour depends on topological rather than metric distance: Evidence from a field study*, Proc. Natl. Acad. Sci. USA, 105 (2008), pp. 1232–1237.

[8] A. J. Bernoff and C. M. Topaz, *A primer of swarm equilibria*, SIAM J. Appl. Dyn. Syst., 10 (2011), pp. 212–250.

[9] A. L. Bertozzi, J. A. Carrillo, and T. Laurent, *Blow-up in multidimensional aggregation equations with mildly singular interaction kernels*, Nonlinearity, 22 (2009), pp. 683–710.

[10] A. L. Bertozzi, T. Laurent, and F. Léger, *Aggregation and spreading via the Newtonian potential: The dynamics of patch solutions*, Math. Models Methods Appl. Sci., 22 (2012), 1140005.

[11] A. L. Bertozzi, H. Sun, T. Kolokolnikov, D. Uminsky, and J. H. von Brecht, *Ring patterns and their bifurcations in a nonlocal model of biological swarms*, Commun. Math. Sci., 13 (2015), pp. 955–985.

[12] B. Birnir, *An ODE model of the motion of pelagic fish*, J. Stat. Phys., 128 (2007), pp. 535–568.
[13] A. Blanchet, V. Calvez, and J. A. Carrillo, *Convergence of the mass-transport steepest descent scheme for the subcritical Patlak–Keller–Segel model*, SIAM J. Numer. Anal., 46 (2008), pp. 691–721.
[14] A. Blanchet, J. Dolbeault, and B. Perthame, *Two-dimensional Keller-Segel model: Optimal critical mass and qualitative properties of the solutions*, Electron. J. Differential Equations, 44 (2006), pp. 1–33.
[15] S. Boi, V. Capasso, and D. Morale, *Modeling the aggregative behavior of ants of the species polyergus rufescens*, Nonlinear Anal. Real World Appl., 1 (2000), pp. 163–176.
[16] M. Burger, V. Capasso, and D. Morale, *On an aggregation model with long and short range interactions*, Nonlinear Anal. Real World Appl., 8 (2007), pp. 939–958.
[17] M. Burger, B. Düring, L. M. Kreusser, P. A. Markowich, and C.-B. Schönlieb, *Pattern formation of a nonlocal, anisotropic interaction model*, Math. Models Methods Appl. Sci., 28 (2018), pp. 409–451.
[18] S. Camazine, J.-L. Deneubourg, N. R. Franks, J. Sneyd, G. Theraulaz, and E. Bonabeau, *Self-Organization in Biological Systems*, Princeton University Press, Princeton, NJ, 2003.
[19] J. A. Cañizo, J. A. Carrillo, and F. S. Patacchini, *Existence of compactly supported global minimisers for the interaction energy*, Arch. Ration. Mech. Anal., 217 (2015), pp. 1197–1217.
[20] J. A. Carrillo, M. G. Delgadino, and A. Mellet, *Regularity of local minimizers of the interaction energy via obstacle problems*, Comm. Math. Phys., 343 (2016), pp. 747–781.
[21] J. A. Carrillo, M. Di Francesco, A. Figalli, T. Laurent, and D. Slepčev, *Global-in-time weak measure solutions and finite-time aggregation for nonlocal interaction equations*, Duke Math. J., 156 (2011), pp. 229–271.
[22] J. A. Carrillo, M. Di Francesco, A. Figalli, T. Laurent, and D. Slepčev, *Confinement in nonlocal interaction equations*, Nonlinear Anal., 75 (2012), pp. 550–558.
[23] J. A. Carrillo, L. C. F. Ferreira, and J. C. Precioso, *A mass-transportation approach to a one dimensional fluid mechanics model with nonlocal velocity*, Adv. Math., 231 (2012), pp. 306–327.
[24] J. A. Carrillo, M. Fornasier, J. Rosado, and G. Toscani, *Asymptotic flocking dynamics for the kinetic Cucker–Smale model*, SIAM J. Math. Anal., 42 (2010), pp. 218–236.
[25] J. A. Carrillo, M. Fornasier, G. Toscani, and F. Vecil, *Particle, kinetic, and hydrodynamic models of swarming*, in Mathematical Modeling of Collective Behavior in Socio-Economic and Life Sciences, Model. Simul. Sci. Eng. Technol., Birkhäuser, Boston, 2010, pp. 297–336.
[26] J. A. Carrillo and Y. Huang, *Explicit equilibrium solutions for the aggregation equation with power-law potentials*, Kinet. Relat. Models, 10 (2017), pp. 171–192.
[27] J. A. Carrillo, Y. Huang, and S. Martin, *Explicit flock solutions for quasi-Morse potentials*, European J. Appl. Math., 25 (2014), pp. 553–578.
[28] J. A. Carrillo, Y. Huang, and S. Martin, *Nonlinear stability of flock solutions in second-order swarming models*, Nonlinear Anal. Real World Appl., 17 (2014), pp. 332–343.
[29] J. A. Carrillo, F. James, F. Lagoutière, and N. Vauchelet, *The Filippov characteristic flow for the aggregation equation with mildly singular potentials*, J. Differential Equations, 260 (2016), pp. 304–338.
[30] J. A. Carrillo, R. J. McCann, and C. Villani, *Kinetic equilibration rates for granular media and related equations: Entropy dissipation and mass transportation estimates*, Rev. Mat. Iberoam., 19 (2003), pp. 971–1018.
[31] J. A. Carrillo, R. J. McCann, and C. Villani, *Contractions in the* 2*-Wasserstein length space and thermalization of granular media*, Arch. Ration. Mech. Anal., 179 (2006), pp. 217–263.
[32] A. Cavagna, A. Cimarelli, I. Giardina, G. Parisi, R. Santagati, F. Stefanini, and R. Tavarone, *From empirical data to inter-individual interactions: Unveiling the rules of collective animal behavior*, Math. Models Methods Appl. Sci., 20 (2010), pp. 1491–1510.
[33] P. Degond and S. Motsch, *Large scale dynamics of the persistent turning Walker model of fish behavior*, J. Stat. Phys., 131 (2008), pp. 989–1021.
[34] A. M. Delprato, A. Samadani, A. Kudrolli, and L. S. Tsimring, *Swarming ring patterns in bacterial colonies exposed to ultraviolet radiation*, Phys. Rev. Lett., 87 (2001), 158102.
[35] M. R. D'Orsogna, Y. L. Chuang, A. L. Bertozzi, and L. S. Chayes, *Self-propelled particles with soft-core interactions: Patterns, stability, and collapse*, Phys. Rev. Lett., 96 (2006), 104302.

[36] B. Düring, C. Gottschlich, S. Huckemann, L. M. Kreusser, and C.-B. Schönlieb, *An anisotropic interaction model for simulating fingerprints*, J. Math. Biol., 78 (2019), pp. 2171–2206.
[37] L. Edelstein-Keshet, J. Watmough, and D. Grunbaum, *Do travelling band solutions describe cohesive swarms? An investigation for migratory locusts*, J. Math. Biol., 36 (1998), pp. 515–549.
[38] K. Fellner and G. Raoul, *Stable stationary states of non-local interaction equations*, Math. Models Methods Appl. Sci., 20 (2010), pp. 2267–2291.
[39] K. Fellner and G. Raoul, *Stability of stationary states of non-local equations with singular interaction potentials*, Math. Comput. Modelling, 53 (2011), pp. 1436–1450.
[40] R. C. Fetecau, Y. Huang, and T. Kolokolnikov, *Swarm dynamics and equilibria for a nonlocal aggregation model*, Nonlinearity, 24 (2011), pp. 2681–2716.
[41] M. Kücken and C. Champod, *Merkel cells and the individuality of friction ridge skin*, J. Theoret. Biol., 317 (2013), pp. 229–237.
[42] T. Kolokolnikov, J. A. Carrillo, A. Bertozzi, R. Fetecau, and M. Lewis, *Emergent behaviour in multi-particle systems with non-local interactions [editorial]*, Phys. D, 260 (2013), pp. 1–4.
[43] T. Kolokolnikov, H. Sun, D. Uminsky, and A. L. Bertozzi, *Stability of ring patterns arising from two-dimensional particle interactions*, Phys. Rev. E (3), 84 (2011), 015203.
[44] H. Li and G. Toscani, *Long-time asymptotics of kinetic models of granular flows*, Arch. Ration. Mech. Anal., 172 (2004), pp. 407–428.
[45] A. Mogilner and L. Edelstein-Keshet, *A non-local model for a swarm*, J. Math. Biol., 38 (1999), pp. 534–570.
[46] A. Mogilner, L. Edelstein-Keshet, L. Bent, and A. Spiros, *Mutual interactions, potentials, and individual distance in a social aggregation*, J. Math. Biol., 47 (2003), pp. 353–389.
[47] A. Okubo and S. A. Levin, *Diffusion and Ecological Problems*, in Interdisciplinary Applied Mathematics: Mathematical Biology, Springer, New York, 2001, p. 197–237.
[48] J. K. Parrish and L. Edelstein-Keshet, *Complexity, pattern, and evolutionary trade-offs in animal aggregation*, Science, 284 (1999), pp. 99–101.
[49] I. Prigogine and I. Stenger, *Order Out of Chaos*, Bantam Books, New York, 1984.
[50] G. Raoul, *Non-local interaction equations: Stationary states and stability analysis*, Differential Integral Equations, 25 (2012), pp. 417–440.
[51] R. Simione, *Properties of Minimizers of Nonlocal Interaction Energy*, PhD thesis. Carnegie Mellon University, Pittsburgh, PA, 2014.
[52] C. M. Topaz and A. L. Bertozzi, *Swarming patterns in a two-dimensional kinematic model for biological groups*, SIAM J. Appl. Math., 65 (2004), pp. 152–174.
[53] C. M. Topaz, A. L. Bertozzi, and M. A. Lewis, *A nonlocal continuum model for biological aggregation*, Bull. Math. Biol., 68 (2006), pp. 1601–1623.
[54] C. Villani, *Topics in Optimal Transportation*, Grad. Stud. Math., American Mathematical Society, Providence, RI, 2003.
[55] J. H. von Brecht and D. Uminsky, *On soccer balls and linearized inverse statistical mechanics*, J. Nonlinear Sci., 22 (2012), pp. 935–959.
[56] J. H. von Brecht, D. Uminsky, T. Kolokolnikov, and A. L. Bertozzi, *Predicting pattern formation in particle interactions*, Math. Models Methods Appl. Sci., 22 (2012), 1140002.